Westinghouse

Westinghouse Electric Company
Nuclear Services
P.O. Box 355
Pittsburgh, Pennsylvania 15230-0355
USA

U.S. Nuclear Regulatory Commission
Document Control Desk
Washington, DC 20555-0001

Direct tel: (412) 374-4643
Direct fax: (412) 374-4011
e-mail: greshaja@westinghouse.com

Our ref: LTR-NRC-05-26

Attn: J. S. Wermiel, Chief
Reactor Systems Branch
Division of Systems Safety and Analysis

May 18, 2005

Subject: Westinghouse Responses to NRC Request for Additional Information (RAIs) on "Optimized ZIRLO™" Topical – Addendum 1 to WCAP-12610-P-A and CENPD404-P-A (Non-Proprietary), TAC No. MB8041

Dear Mr. Wermiel:

Enclosed is one (1) copy of Westinghouse Responses to NRC Request for Additional Information (RAIs) on "Optimized ZIRLO™" Topical – Addendum 1 to WCAP-12610-P-A and CENPD404-P-A (Non-Proprietary) dated May 2005, TAC No. MB8041. The proprietary version of these responses were transmitted in LTR-NRC-04-44 dated August 4, 2004. A non-proprietary version of the responses is being sent as requested by the NRC.

Very truly yours,

J. S. Galembush, Acting Manager
Regulatory Compliance and Plant Licensing

Enclosures

cc: F. M. Akstulewicz/NRR
P. M. Clifford/NRR
B. J. Benney/NRR

ZIRLO™ trademark property of Westinghouse Electric Company LLC

COPYRIGHT NOTICE

Westinghouse Responses to NRC Request for Additional Information (RAIs) On Optimized ZIRLO™ Topical – Addendum 1 to WCAP12610-P-A and CENPD404-P-A

(for Proprietary Class 2 Refer to LTR-NRC-04-44, August 4, 2004)

Westinghouse Electric Company LLC
P.O. Box 355
Pittsburgh, PA 15230-0355

Westinghouse Responses to NRC Request for Additional Information (RAIs) On Optimized ZIRLO™ Topical – Addendum 1 to WCAP12610-P-A and CENPD404-P-A

1. Section 1.2 provides a definition of ZIRLO™ material based upon descriptions presented in both the "NRC SE and Appendix A of WCAP-12610, and also accounting for descriptions of ZIRLO™ in patent documents". The table below lists the alloy content of ZIRLO™ found in these sources.

   Response 1:
   ZIRLO™ is a trademark commercially used by Westinghouse in connection with zirconium based alloys containing about 1% niobium (together with smaller amounts of iron and tin and other elements) and having a particular microstructure. The Abstract of US Patent No. 4,649,023 discusses zirconium alloys containing 0.5 to 2.0 percent niobium and "up to 1.5 percent tin". Westinghouse has the following patents relating to specific compositions and/or processing: 4,649,023; 5,112,573; 5,125,985, 5,266,131 and 5,230,758. There is not a direct correspondence between the licensed alloy range and the alloy range of a specific patent. The patents are used for commercial protection and are not used to define a basis for a license composition.

   a. Explain the differences in alloying content and why Optimized ZIRLO™ is within the definition of ZIRLO™ material.

   Response 1a:
   The difference in alloy content between the current ZIRLO™ and Optimized ZIRLO™ is the tin level. All other alloying additions remain within the current licensed ranges. ZIRLO™ is an alloy containing 98 % zirconium with added elements of niobium, tin, and iron. An important characteristic of ZIRLO™ is the type of precipitates that are formed in the alloy. Since the precipitates consist of niobium and iron with zirconium and not with tin, the small changes in tin content do not affect the precipitate structure.

b. Explain why do the nickel and chromium alloying content remain in the patented description of ZIRLO™?

Response 1b:
The patents do not provide a definition of ZIRLO™. As stated above, patents provide commercial protection for a broader alloy range than the licensed version of ZIRLO™.

c. Will the ZIRLO™ patent be revised to reflect the Addendum 1 alloy content?

Response 1c:
There is no need to revise the above mentioned patents. They will not be revised.

d. A definition of ZIRLO™ is presented in quotation marks in Section 1.2. What is the source of this quote?

Response 1d:
The description quoted was developed by Westinghouse to provide a clear statement of the unique characteristics that define ZIRLO™ and is consistent with WCAP 12610. Optimized ZIRLO™ will continue to be within the definition of ZIRLO™.

2. The material properties of a metal alloy are strongly dependent on its microstructure, which is influenced by both alloy content and material processing.

Response 2:

[

] a,c

a. Describe, in detail, each step of the current material processing employed to dictate the microstructure of ZIRLO (e.g. annealing temperature, beta quench, cold work, age hardening, etc.).

Response 2a:

ZIRLO is processed similar to Zircaloy 4. [

] a,c

b. How will the current process described above be altered for Optimized ZIRLO?

Response 2b:

The same basic processing steps used in the production of ZIRLO will be used for Optimized ZIRLO. The equivalent product can be manufactured using different processing parameters so it is important not to assume a specific process route is the only acceptable route. [

] a,c

c. Describe the Quality Control procedures on the control of microstructure (e.g. alloy content, size and distribution of second phase particles, grain size, etc.).

Response 2c:

[

] [a,c] **The established process parameters are monitored by Quality Control in addition to the standard property testing of the final product required by the specifications. Typically, alloy content is verified on each ingot by chemistry measurements, and an in-direct method of monitoring the microstructure involving physical and mechanical testing of the final product is used.**

d. Quantify the allowed manufacturing tolerances on alloy content and the control of microstructure?

Response 2d:

Alloy Composition

The alloy content tolerances are established and controlled by the applicable material specifications. The range in alloy chemistry for Optimized ZIRLO is listed in Table 2.D.1.

Table 2.D.1 - Optimized ZIRLO Cladding Composition

Element	Nominal value (wt%)	Allowable range (wt%)
Niobium	[ ] [a,c]	0.8 - 1.2
Iron	[ ] [a,c]	0.09 – 0.13
Tin	[ ] [a,c]	0.6 – 0.8
Oxygen	[ ] [a,c]	0.09 – 0.16
Zirconium	[ ] [a,c]	Balance
Trace element levels	Typical of Zircaloy 4 – ASTM B 811	

Mechanical Properties

The product specifications include acceptance criteria for the tensile strength and ductility of Optimized ZIRLO components. The mechanical strength of the material is controlled also by process procedures and qualifications and verified by quality control testing. Table 2.D.2 lists basic mechanical properties that encompass Optimized ZIRLO cladding. Additional data on the mechanical test results on Optimized ZIRLO is reported in Section B.7 of Addendum 1 to WCAP 12610-P-A

a,b,c

Table 2.D.2 Room Temperature Tensile Values

[

]

Physical Properties

Addendum 1 to WCAP 12610-P-A contains extensive lists of physical property data obtained from testing of Optimized ZIRLO. There are primarily two physical properties that are monitored during the production of Optimized ZIRLO cladding; hydride orientation and autoclave performance. The hydride orientation is measured using ASTM B811 as a guideline and the maximum value of [ ]^{a,c} is applied to the test results for Optimized ZIRLO. The autoclave testing is done over a test time of three days in [

]^{a,c}

The precipitate microstructure is controlled by the qualified processing parameters. The anneal times and temperatures are controlled to insure adequate formation and aging of the precipitate microstructure. For ZIRLO the precipitate size is maintained relatively small compared to Zircaloy 4. Since the precipitate size and chemistry is a function of the iron and niobium levels in ZIRLO and these elements are present in Optimized ZIRLO at the same levels as in standard ZIRLO ; thus, the precipitate microstructure in Optimized ZIRLO is the same as in ZIRLO and is described below:

[

]^{a,c}

3. Irradiation experience with Optimized ZIRLO™ is discussed in Section 3.5.
   a. In light of the limited database presented, justify the material properties up to 62,000 MWD/MTU.

Response 3a:

The characterization testing reported in the addendum demonstrates that standard ZIRLO material properties currently used in various models and methodologies are applicable to analyses of Optimized ZIRLO. The primary effects of a reduced tin level in ZIRLO are a minor reduction in the un-irradiated mechanical strength and improvement in the corrosion resistance. The higher burn-up levels are associated with higher fluence levels. Since the precipitate structure remains the same for current and Optimized ZIRLO, the past performance of ZIRLO precipitate structure at high burn-ups also is similar to the Optimized ZIRLO condition.

Likewise, with the irradiation strengthening occurring during the initial irradiation, the Optimized ZIRLO performance will be the same as the current ZIRLO performance. The irradiation strengthening that occurs with the initial fuel operation negates the starting differences in mechanical strength. This effect has been reported in the general literature. An early example is found in ASTM STP 681 in an article by K. Pettersson on the effects of irradiation on the mechanical strength of Zircaloy tubes. Figure 3.1 is a copy of one of the figures in the report that shows that irradiation strengthening occurs very early in the initial operating cycle. The data shows that there is an initial period when at relatively low fluence (3×10^{21} n/cm^2) the majority of the irradiation strengthening occurs. Data reported in ASTM STP 484 by D.H. Hardy on "The Effect of Neutron Irradiation on the Mechanical Properties of Zirconium Alloy Fuel Cladding in Uniaxial and Biaxial Tests" indicates that (a) strengthening occurs during the initial

irradiation, (b) for large differences in starting conditions the strength differences are not fully eliminated at 3 x 10^{21} n/cm^2 and (c) after about 3 x 10^{21} n/cm^2 the 0% cold worked structure has a strength similar to the un-irradiated cold worked material. Information from hot cell testing of irradiated thimble tubes and cladding confirms the effects of irradiation strengthening in reducing/negating the strength differences initially present in the starting un-irradiated material. Due to processing differences the standard ZIRLO thimble tubes have a lower un-irradiated strength [ ]$^{a, b, c}$ compared to un-irradiated fuel cladding. As shown in the data table included in the response to RAI #25, measured strengths of cladding and thimble tubes show a significant difference in un-irradiated strengths but upon irradiation the mechanical strengths of both the thimble tube and the cladding are increased to similar levels. The difference in un-irradiated mechanical strengths between Standard ZIRLO and Optimized ZIRLO is much less than the corresponding difference between cladding and thimbles. The strength increase due to irradiation is generally beneficial and provides additional margin between stress and stress criteria.

Figure 3.1 Effects of Fluence Levels on Mechanical Properties (ASTM STP 681 - article by K.Pettersson)

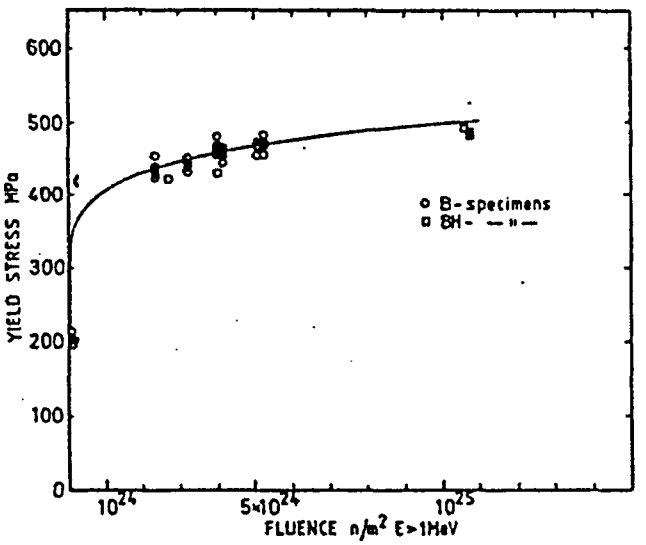

FIG. 2—*Fluence dependence of the yield stress for the B specimens.*

The difference in corrosion resistance is not changed with irradiation and is a positive result. The corrosion resistance comes primarily from both the precipitate microstructure and the tin levels. As indicated in earlier responses the precipitate structure in Optimized ZIRLO is the same as the standard ZIRLO, so there will be no difference in performance related to the precipitate structure. However, past experience with low tin Zircaloy-4 and associated alloys indicates that the tin level reduction results in a lower (beneficial) corrosion rate. This has been confirmed during the second cycle of operation in [ ]^{a,c} where the oxide thickness on the Optimized ZIRLO cladding continues to show significant improvements over the Standard ZIRLO cladding. Oxide reductions exceeding 20% have been measured for Optimized ZIRLO compared to standard ZIRLO on the [ ]^{a,c} LTA rods after 52 GWD/MTU.

Figure 3.2

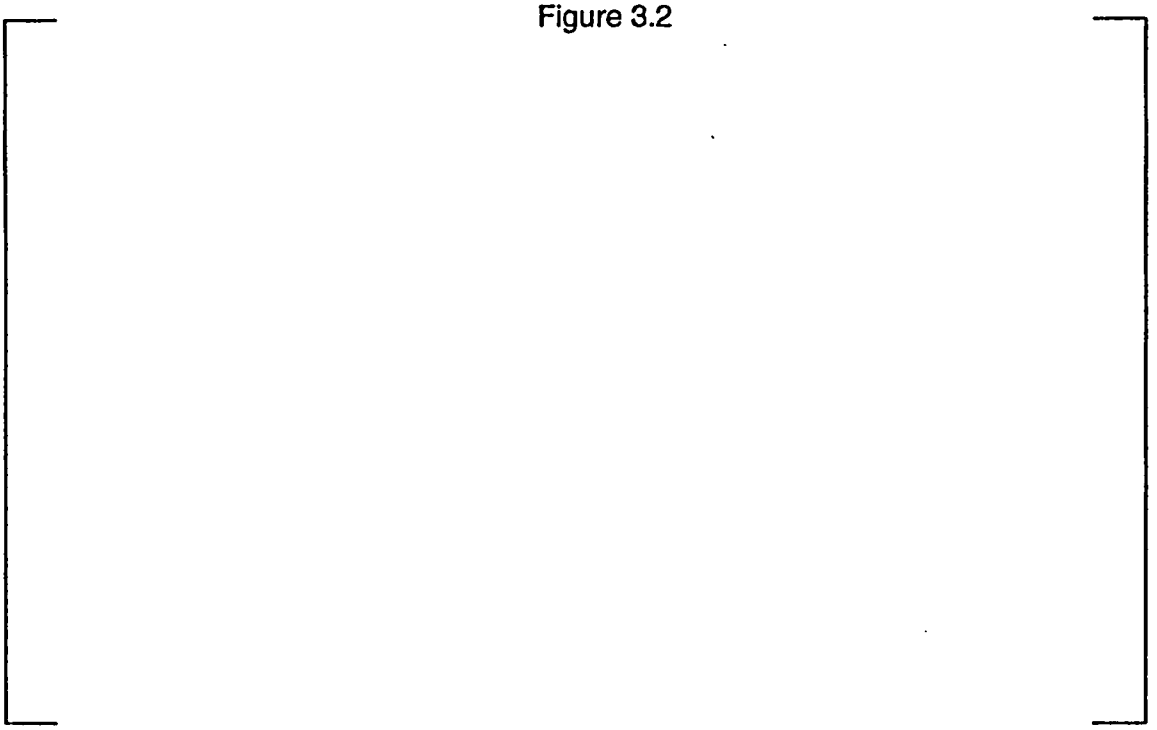

a,b,c

b. Exemptions for LTAs containing Low-Tin ZIRLO™ have been issued for several plants. When will data be available for clad material approaching 0.60 w/o tin and 62,000 MWD/MTU?

The following is a summary of Low Tin Zirlo™ LTA programs and summary of available data from the Byron LTA program

Byron

Two characterized LTAs containing Optimized ZIRLO cladding were inserted into Byron Unit 1 Cycle 10. After Unit 1 Cycle 10 the LTAs were discharged to the SFP for interim examinations in December of 2000. The LTAs were subsequently reinserted into Byron Unit 2 Cycle 10 for an additional cycle. The LTAs were once again discharged for interim examinations in October 2002. After the exams the LTAs are schedule to be reinserted into Unit 1 Cycle 13 to achieve peak rod burnup in excess of 62,000 GWD/MTU.

The interim examinations for the Byron LTAs included measurements of overall assembly growth, individual fuel rod growth and structural corrosion as well as other pool-side examinations. The results of the Optimized ZIRLO measurements from the end of the first and second cycles are shown in Table 3-1 below along with Standard ZIRLO peak oxide data for comparison purposes. To date the Optimized ZIRLO cladding has exhibited excellent corrosion

performance in the Byron LTAs while fuel rod and assembly growth remain within the existing ZIRLO database.

a, b, c

At the conclusion of the Byron LTA program several Optimized ZIRLO fuel rods with varying degrees of burnup will be available for more extensive study.

Calvert Cliffs

Four LTAs containing a variety of advanced cladding alloys including Optimized ZIRLO were inserted into the Calvert Cliffs Unit 2 Cycle 15 core in 2003. These LTAs will be irradiated for two cycles to a burnup less than 60,000 GWD/MTU. The LTAs will be evaluated in a poolside exam after the second cycle and optionally inserted into Calvert Cliffs Unit 1 Cycle 19 for a third cycle to generate additional high burnup data. The first cycle of irradiation for these LTAs is currently underway.

Catawba

Eight characterized LTAs containing Optimized ZIRLO cladding were inserted in the Catawba Unit 1 Cycle 15 core at the end of 2003. The LTAs will be examined after each of three cycles. The first cycle of irradiation of these LTAs is currently underway.

Millstone

Eight characterized LTAs containing Optimized ZIRLO cladding were inserted in the Millstone Unit 3 Cycle 10 core for three cycles of irradiation. The LTAs will be examined after each cycle. The first cycle of irradiation of these LTAs began in early 2004.

Schedule for LTA PIE plans is shown in Table 3-2

Table 3-2 LTA PIE plans*

a,c

4. Byron LTAs include Optimized ZIRLO™ thimble tubes. Section 4.4 states, "the use of ZIRLO™ cladding or structural materials for the fuel assembly skeleton...". Is Westinghouse currently using or plan to use either ZIRLO™ or Optimized ZIRLO™ in fuel assembly components other than fuel clad?

Response 4:

Westinghouse is currently using ZIRLO™ in fuel assembly components (thimble tubes and grids). Similarly, Optimized ZIRLO™ has been in use in the Fuel Assembly thimbles and grids in the certain plants currently hosting Optimized ZIRLO™ LTAs. Westinghouse plans to use Optimized ZIRLO™ in fuel assembly components (thimble tubes and grids) upon WCAP approval.

5. With regard to the continued use of Zircaloy-4 properties in the ZIRLO™ models, the SER for CENPD-404-P-A states, "the staff notes that this practice should not be used in the future, and future applications will be expected to fully measure and develop the material properties of proposed new cladding alloys". This Topical Report supports continued use of Zircaloy-4 properties for Optimized ZIRLO™. Please provide the technical bases and relevant data to support your position.

Response 5:

The implementation of standard ZIRLO™ in Combustion Engineering (CE) designed PWRs (CENPD-404-P-A) involved the application of some Zircaloy-4 correlations to standard ZIRLO™ properties because it was demonstrated that the differences were insignificant. However, the Nuclear Regulatory Commission's Safety Evaluation Report (NRC SER) for CENPD-404-P-A noted that this practice should not be used in the future and future applications would be "...expected to fully measure and develop the material properties of proposed new cladding alloys." In this instance, it is important to recognize three Westinghouse considerations in the development of Optimized ZIRLO™ properties.

1. **The first consideration is that Optimized ZIRLO™ is not a new alloy, rather it meets the established definition of ZIRLO™, albeit with a tighter specification on tin content. Consequently, Westinghouse did not consider the SER requirement in this situation to be applicable.**

2. **The second consideration is to note that although the sources of the ZIRLO™ property correlations were identified in CENPD-404-P-A (i.e., as ZIRLO™ or Zircaloy-4), the property was found to be essentially the same for both materials, and the proposed property correlation is a satisfactory correlation for both ZIRLO™ and Zircaloy-4.**

3. **Finally, and most importantly, even though Optimized ZIRLO™ is only a variation of ZIRLO™, Westinghouse developed and performed an extensive and complete test program (described in Appendix A of WCAP-12610-P-A and CENPD-404-P-A Addendum 1) to evaluate the required Optimized ZIRLO™ and standard ZIRLO™ thermal and mechanical properties and compared those properties to approved properties of ZIRLO™ (described in Appendix B of WCAP-12610-P-A and CENPD-404-P-A Addendum 1). It was concluded that the existing property correlations, whether originally from ZIRLO™ or from Zircaloy-4, are, in fact, no less applicable as Optimized ZIRLO™ property correlations. Thus, Westinghouse believes it has conformed to the referenced SER requirement that the properties should be fully measured. Westinghouse concluded, therefore, that the correlations for standard ZIRLO™ in CENPD-404-P-A are also Optimized ZIRLO™ property correlations.**

6. WCAP-12610-P-A Section 2.5.5 addresses fuel clad wear. Why is this design criterion not included for Optimized ZIRLO? Will the models maintain the 10% design wall thickness reduction?

Response 6:

The Fuel Rod Clad Fretting was addressed in our internal Design Review Process. The Criterion, Basis, and Verification for the Fuel Rod Clad Fretting is as follows:

Criterion: Grid assembly springs shall be designed to limit fuel rod clad fretting to less than [ ]$^{a, b, c}$ of the clad wall thickness at the end of fuel assembly life, considering all pertinent factors such as spring relaxation due to irradiation, clad creep-down, grid growth, etc. (There is no change in this criterion).

Basis: Experience has shown that by meeting these spring requirements, excessive fretting of the fuel rod clad is prevented.

Verification: Based on VIPER test results, the fuel rods of ZIRLO™ material has demonstrated fretting wear resistance that is equal to or better than the fuel rods with Zircaloy-4 material. VIPER tests conducted on Optimized ZIRLO™ also met the fretting wear resistance criteria. As the reactor starts operation, an oxide film forms on both the spring and rod surfaces. It is these surfaces that are subject to any potential fuel clad wearing. Both surfaces are zirconium oxide and there are no expected differences in the

Optimized ZIRLO™ oxide characteristic. Hence the wear rate for the Optimized ZIRLO™ fuel rods is expected to be comparable to the ZIRLO™ material. Therefore, the design criterion is satisfied.

7. The evaluation of DNB propagation in Section 4.2.1 concludes that since there is no effect on rod internal pressure, there will be no effect on DNB propagation.

a. The extent of DNB propagation would also depend on material properties (e.g., creep) and this needs to be addressed.

b. The criteria states that the internal pressure of the lead fuel rod in the reactor will be limited to a value below that which could cause extensive DNB propagation to occur. How is extensive DNB propagation quantified under normal and transient conditions? Are the potential clad failures associated with DNB propagation accounted for in the dose calculations?

Response 7a:

CEN-372-P-A, "Fuel Rod Maximum Allowable Gas Pressure", provides a more comprehensive discussion of DNB propagation than is offered in either WCAP-12610-P-A and CENPD-404-P-A, Addendum 1 or CENPD-404-P-A. Westinghouse agrees that the extent of DNB propagation depends on rod internal pressure and other material properties such as creep. It also depends on operating conditions such as linear heat rate and temperature of the cladding which, in turn, depends on the duration of the time in DNB, coolant temperature and pressure conditions, waterside corrosion and cladding loss, and the amount of rod-to-rod gap closure during a DNB transient. The evaluation in WCAP-12610-A and CENPD-404-P-A Addendum 1, Section 4.2.1, includes these dependencies as well as the potential distribution of fuel rods in DNB and above the reactor system coolant pressure. Since there is no effect of Optimized ZIRLO™ on normal plant operation, no effect on the individual DNB transient behavior relative to standard ZIRLO™, and no difference from ZIRLO™ material properties, there will be no effect on the distribution of fuel rod internal pressures relative to the distribution of fuel rods experiencing DNB during a DNB transient. As a result, there is no effect on the extent of DNB propagation. The only effect would be from reduced waterside corrosion and, therefore, reduced clad thinning and reduced creep, which would have a beneficial effect. This beneficial effect is ignored. Since this is not credited in the analyses, the result is no effect on DNB or DNB propagation.

Response 7b:

A specific limit on the fraction of rods allowed to experience DNB due to propagation is based on requiring that the total number of rods in DNB , including DNB propagation effects are within the limits for rod failure by DNB assumed in the offsite dose limit calculations. DNB propagation analyses are performed for each Condition III/IV DNB event identified. Typically, these events include: Single Rod Withdrawal at Power, Ejected Rod, and Locked Rotor. The actual number of rods allowed in DNB for each analysis is confirmed in the evaluation. Therefore, the clad failures associated with DNB propagation are bounded by the dose calculations.

8. WCAP-12610-P-A Section 2.5.3 lists a temperature limit for Condition I which differs from the corresponding value in Addendum 1. Is this a planned change to the criteria or a typo?

Response 8:

Yes, this is a typographical error; WCAP-12610-P-A Section 2.5.3 lists the correct temperature limit of 780 °F for Condition I. A correction will be made to the approved report WCAP-12610-P-A and CENPD-404-P-A Addendum 1.

9. Section 4.2.2 makes a statement concerning the "...continued use of Standard ZIRLO™ properties and models for Optimized ZIRLO™...". Identify when properties and models are based upon which clad material (e.g., Standard ZIRLO™, Optimized ZIRLO™, Zircaloy-4).

Response 9:

The Optimized ZIRLO™ measured properties and, therefore, model correlations, have been demonstrated to be equivalent to standard ZIRLO™ in Appendix B of WCAP-12610-P-A and CENPD-404-P-A Addendum 1. The implementation of standard ZIRLO™ in CE designed PWRs (see CENPD-404-P-A) involved the application of some Zircaloy-4 correlations to standard ZIRLO™ properties because it was demonstrated to be appropriate. This approach was accepted by the NRC as part of the review and approval of CENPD-404-P-A, as documented in the SER. The identification of when the source of property and model correlations were ZIRLO™ or Zircaloy-4 (OPTIN™) is summarized in CENPD-404-P-A Appendix A, Tables 7 through 25.

As stated in Response 5, however, it is concluded that the existing property correlations, whether originally from ZIRLO™ or from Zircaloy-4, are, in fact, directly applicable for use as Optimized ZIRLO™ properties.

10. Section 4.2.2 states that the calculation of DNB propagation depends on internal rod pressure, high temperature creep, and high temperature burst stress. Do DNB propagation calculations predict clad burst under non-LOCA transient conditions? If so, provide information on how the potential impacts of this failure mechanism have been addressed within the respective events dose calculation.

Response 10:

Under certain non-LOCA transient conditions, DNB propagation calculations may predict cladding burst. If clad burst is predicted, the fuel rod internal pressure is relieved and no further cladding strain occurs. The dose contribution from the burst fuel rod is automatically accounted for in the dose calculation because it was already in DNB and, consequently, conservatively assumed to fail regardless of whether or not burst was actually predicted.

11. With regard to potential differences between tensile and compressive creep rates and the "relatively small creep database for ZIRLO™", the SER for CENPD-404-P-A states, "WEC committed to acquire more in-reactor creep data under both tensile and compressive stress conditions for ZIRLO™ material". The SER concludes, "On the basis of the approved creep model and the commitment to acquire additional data, the staff considers that the creep model for the NCLO criterion is acceptable for FATES3B".

    a. What is the current status of the "detailed irradiation program for ZIRLO™"?

    Response 11a:
    A detailed irradiation growth and creep program initiated irradiation in Vogtle unit 2 cycle 10 in November 2002. The first test assembly is scheduled to be discharged at the end of cycle 10 in May 2004.

    b. Addendum 1 states, "An evaluation demonstrated that the application of Standard ZIRLO™ properties and models to Optimized ZIRLO™ will have no impact on maximum internal pressure and will have a conservative impact on the NCLO critical pressure limit". Did this evaluation consider in-reactor creep data from the above commitment?

    Response 11b:
    The in-reactor creep data from the above commitment is not yet available and thus was not used in the evaluation. The evaluation was based on the same out-reactor thermal creep behavior of Optimized ZIRLO™ and Standard ZIRLO™

12. Section 4.5 of Addendum 1 documents the potential affect of changes in specific heat on Non-LOCA transients.

    a. For all licensees, were all events which experience DNB or elevated clad temperatures evaluated for the further decrease in phase transition temperature (relative to both Zircaloy-4 and Standard ZIRLO™)?

    b. Provide a list of the events considered and the calculated peak clad temperature for each event.

    c. Was FACTRAN and/or STRIKIN-II used to calculate peak clad temperature for Locked Rotor/Sheared Shaft as well as any other event which experienced DNB or elevated clad temperatures?

Westinghouse Plants

Response:

The Peak Cladding Temperatures (PCT) calculated in a number of FSAR analyses for 2, 3, and 4-loop plants were reviewed as part of the Standard ZIRLO™ licensing effort. It was found that the cladding temperature remains below the phase transition temperature (~1400°F) for the following events:

- **RCCA Withdrawal from Subcritical**
- **RCCA Withdrawal at Power**
- **Dropped RCCA/RCCA Bank Event**
- **Boron Dilution (all modes)**
- **Startup of an Inactive Reactor Coolant Loop**
- **Loss of Electrical Load and Turbine Trip**
- **Loss of Normal Feedwater and Station Blackout**
- **Excessive Heat Removal Due to Feedwater Malfunction**
- **Excessive Load Increase**
- **Accidental Depressurization of the Reactor Coolant System**
- **Steamline Break (core response and mass & energy release, at all power levels)**
- **Complete Loss of Flow**
- **Partial Loss of Flow**
- **Main Feedline Rupture**

The only events that result in PCTs higher than the phase transition temperature are Locked Rotor and RCCA Ejection (Hot Full Power and Hot Zero Power cases).

For these events, sensitivity studies using the FACTRAN code were completed to quantify the effect of the change in specific heat between Standard ZIRLO™ and Zircaloy-4. The sensitivity studies showed that the difference in specific heat between Zircaloy-4 and Standard ZIRLO™ has very little effect (~2°F in PCT) on the results. These results were judged to be applicable to Optimized ZIRLO™ since the specific heats of Standard and Optimized ZIRLO™ are the same within the accuracy of the data.

The PCTs calculated in the Locked Rotor and Rod Ejection analyses considered in the sensitivity studies are shown in Table 1 below.

[

] a, b, c

CE Plants

Response 12a:

CENPD-404-P-A, Rev 0, "Implementation of ZIRLO™ Cladding Material in CE Nuclear Power Fuel Assembly Designs", November 2001, concluded that, with respect to cladding materials, only specific heat was of importance to one computer code used for non-LOCA analysis. Other computer codes are not sensitive to clad material properties, or the models used are adequate for modeling ZIRLO™. This was true for thermal conductivity where it was shown that Zircaloy-4 and ZIRLO™ have the same thermal conductivity equations. The one computer code that was impacted was the STRIKIN-II code used to perform CEA Ejection analysis. As discussed in CENPD-404-P-A, CEA Ejection is impacted because it is the only event that has the potential for exceeding the ZIRLO™ lower alpha-beta phase change temperature. Up to the phase change temperature, ZIRLO™ and Zircaloy-4 have virtually identical specific heat curves. After passing through the phase change temperature, the specific heats change and this could impact STRIKIN-II predicted total hot spot deposited energy (the acceptance criteria for CEA Ejection). For this reason STRIKIN-II and CEA Ejection were investigated. Analysis was performed for CENPD-404-P-A to quantify the impact on CEA Ejection results using ZIRLO™ specific heat inputs to STRIKIN-II. This was done for both CE 14x14 and 16x16 fuel designs. The conclusion presented in CENPD-404-P-A is that the impact is negligible

For the Optimized ZIRLO™ report, an evaluation was performed to determine the impact of the slightly lower phase change temperature of Optimized ZIRLO™. The evaluation (which relied on STRIKIN-II results using Zircaloy-4 and ZIRLO™ properties) found that the Optimized ZIRLO™ and ZIRLO™ specific heat are very similar up to the alpha-beta phase change temperature of Optimized ZIRLO™ (approximately 1250 °F vs 1380 °F for ZIRLO™). Additionally, the data indicates that Optimized ZIRLO™ and Zircaloy-4 are much more nearly equal than are Zircaloy-4 and ZIRLO™ during the phase change. Consequently, it was concluded that the impact of Optimized ZIRLO™ relative to ZIRLO™ was again negligible.

Response 12b:

CENPD-404-P-A, Table 7.3-1 provides a list of events considered. Since the Optimized ZIRLO™ properties are the same as ZIRLO™, the peak clad temperatures will be the same as CENPD-404-P-A, Section 7.3.

Response 12c:

FACTRAN and STRIKIN-II are used to calculate peak clad temperature for DNB events. FACTRAN is used by Westinghouse on Westinghouse designed PWRs and STRIKIN-II is used by Westinghouse on CE designed PWRs.

13. ZIRLO™ alloy is described as having a "...microstructure comprising second phase precipitates (specifically, a body-centered cubic beta-niobium-zirconium phase and a hexagonal zirconium-niobium-iron inter-metallic phase) homogeneously distributed throughout the zirconium matrix."

a. Describe how the reduction in tin will influence the shape, size, distribution, and weight fraction of the second phase precipitates (beta-ZrNb and hcp-ZrNbFe).

Response 13a:

The two precipitate phases do not contain tin and thus their shape, size, distribution and weight fractions are not affected by the reduction in tin.

b. Describe how planned changes to the material processing will influence the shape, size, distribution, and weight fraction of the second phase precipitates (beta-Zr-Nb and hcp-Zr-Nb-Fe).

Response 13b:

The second phase or precipitate characteristics are a function primarily of the relative levels of niobium and iron in the alloy. The impacts of the process are focused on the reaching a near equilibrium condition in the precipitate microstructure. The Optimized ZIRLO™ processing follows the past ZIRLO™ processing and minor change in past ZIRLO™ annealing temperatures will not impact shape, distribution, size and weight fraction of the precipitates in Optimized ZIRLO™ compared to past ZIRLO™ production.

14. Sections 2.2 and 3.1 – It appears the mean tin content for Optimized ZIRLO™ will be around [ ]^{a,c}? Is this interpretation correct? To what tolerance limit will the [ ]^{a,c} value be applied in the fabrication of Optimized ZIRLO™?

Response 14:

The target tin content in Optimized ZIRLO™ will be [ ]$^{a, b, c}$ with lower limit of 0.6% and [ ]$^{a, b, c}$. The test lot was fabricated with a target tin content of 0.6% to respond to NRC's concern to make certain that the characterization data bounds the desired [ ]$^{a, b, c}$ tin lower limit for Optimized ZIRLO™

15. Please provide the fabrication differences between the standard ZIRLO™, standard Zr-4, low tin Zr-4, and Optimized ZIRLO™ for cladding and guide tubes. This includes the intermediate cold-work and annealing steps but of particular interest is the final cold-work, annealing temperatures and times. If the annealing times have changed between the materials please provide the average grain size for the Standard and Optimized ZIRLO™ and any texture differences. Also what are the fabrication specifications for the Standard and Optimized ZIRLO™.

Response 15:

The basic fabrication difference in the production cycle for these materials is at the alloy additions for the ingot melting. At this stage all of the materials have different mixes of elements added to the electrode. This is the stage where the different tin levels between standard and Optimized ZIRLO are controlled. The processing of thimble tubes and cladding is the same until near the final pilger reductions. At the final stages there are differences in size reduction (cold working during pilgering and dash pot forming in the thimble tubes). For Zircaloy-4 cladding the final anneal has included both SRA and partial recrystallization anneals depending on the particular design requirements. Changes inherent in process improvements have occurred over time with both the ZIRLO and Zircaloy-4 tube production.

Tubing has been produced by four different vendors and each of the suppliers have had a mildly different process. The initial ZIRLO ingot was made by a Wah Chang process. Subsequent ingots have been made by Western Zirconium. At the Westinghouse Specialty Metals Plant the ZIRLO processing has gone through multiple optimizations, and the current process

modification is referred to as the sixth route. Sandvik Special Metals has also produced ZIRLO tubing using their specific process. The tubing characteristics from the various processes were controlled to meet the design requirements by specifications, drawings, process controls, and quality control testing.

Annealing of Intermediate and Final Tubes:

Because Optimized ZIRLO has a reduced tin level and tin is an alpha stabilizer, there is a resultant small reduction in the phase transition temperature as reported in WCAP-12610-P-A and CENPD-404-P-A Addendum 1. The transition temperature effect combined with the data that shows improved corrosion resistance with lower temperature intermediate annealing indicates that improved corrosion performance of ZIRLO alloys can be achieved with minor modifications to the annealing parameters while still maintaining the required material design characteristics. Process changes of this type are implemented per normal practice when fully qualified. Also since tin provides a degree of creep strengthening, the reduced tin alloy has lower creep strength. A recovery of creep strength can be gained by anneal and/or cold working changes. For the current Optimized ZIRLO process the final anneal temperature has been increased by [ ]$^{a, b, c}$ to offset the creep strength reduction from the lower tin.

Cold Work and Grain Size:

[

]^{a,c}

Tubing Texture:

CSR is a measure of the tubing texture and the same CSR limits apply for ZIRLO and Optimized ZIRLO™ in the current tubing specifications. Texture measurements for Optimized ZIRLO are also reported in WCAP-12610-P-A and CENPD-404-P-A Addendum 1.

Process Specifications:

More important than the specific process a variable is that the final product is within the required alloy property ranges that are reflected in the models and design codes. These properties are monitored and controlled by the process qualifications, the design drawings and the product specifications along with other characterization tests. Westinghouse does not have a process specification for fuel cladding. The cladding specification identifies most of the key material characteristic ranges, and the production facilities develop process plans that define a set of process parameters that will be used to fabricate the cladding to meet the specification and drawing requirements.

16. Section 4.6 (Page 20) – It is stated both the ZIRLO™ specific heat model used in WCOBRA/TRAC and the specific heat approximation used in HOTSPOT compared to the differences in the new specific heat data have a negligible affect on large break LOCA analyses even though there is a [ ]^{a,c} difference between the models and the data within a [ ]^{a,c} range. Please discuss further how the sensitivity analysis was performed and the results of the analysis that compare the ZIRLO™ model to the Optimized ZIRLO™ data. Also, explain the differences between the specific heat model in WCOBRA/TRAC and the approximation used in HOTSPOT. (Page 28) An argument is made for the CE evaluation model such that the [ ]^{a,c} higher specific heat for the model compared to the Optimized ZIRLO™ data within the [ ]^{a,c} range will not have a significant impact on peak cladding temperature for LBLOCA but no sensitivity analysis is provided to substantiate this claim. Please provide a sensitivity analysis that demonstrates that the overprediction of specific heat has no or an insignificant effect on LBLOCA results.

Westinghouse Response 16:

The model used in WCOBRA/TRAC for ZIRLO™ cladding specific heat is given in Table 10-18 of Reference 16-1, and is approximated as follows in HOTSPOT:

[

]^{a,b,c}

Linear extrapolation of the first two points is used below 300 K, and linear interpolation of the neighboring points is used for intermediate values. As shown in Figure 16-1, there are only minor differences between the two models, indicating that the simplified model used in HOTSPOT is adequate for the intended purpose.

Figure 16-1

a, b, c

For the HOTSPOT sensitivity calculation described in Section 4.6.1 of the Topical Report, the ZIRLO™ specific heat model was replaced with a table of 25 points representing the Optimized ZIRLO™ data. These points span the range of the "heating" data from Table B.2-1 of the Topical Report [ ]^{a,b,c} with temperature values chosen to provide a close approximation of the data. Linear extrapolation was used for temperatures outside the data range, and linear interpolation was used for intermediate temperatures. As shown in Figure 16-2, the main differences between the Standard ZIRLO™ model and the 25-point representation of the Optimized ZIRLO™ data occur for temperatures between 1400°F and 1600°F.

Figure 16-2

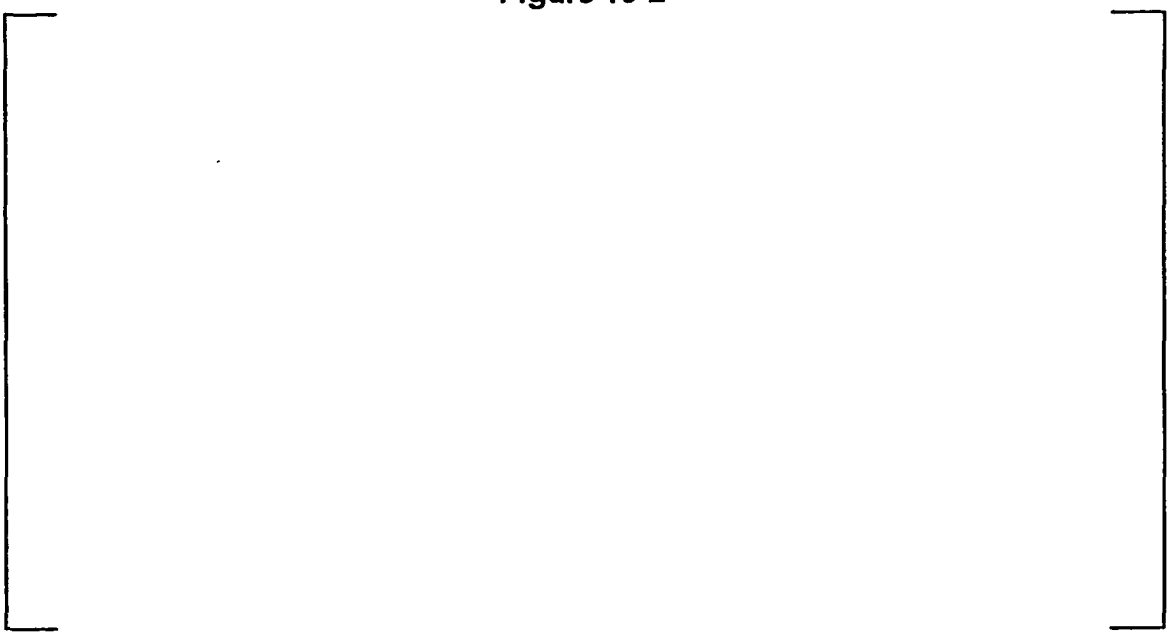

a, b, c

The transient selected for the HOTSPOT sensitivity calculation has a peak cladding temperature (PCT) near the 10 CFR 50.46 limit of 2200°F that occurs early in the reflood phase of the transient. Relative to the Standard ZIRLO™ case, the Optimized ZIRLO™ case showed a 2.7°F increase in average PCT (from 2191.0°F to 2193.7°F) and a 1.7°F decrease in standard deviation (from 54.1°F to 52.4°F) that are considered to be negligible. This is consistent with the expected result, since the differences in specific heat are relatively minor over most of the temperature range of interest for large break LOCA, and since limiting licensing transients spend little time in the temperature range where the most significant differences are observed.

References

16-1. WCAP-12945-P-A Volume I (Revision 2) and Volumes II-V (Revision 1), "Westinghouse Code Qualification for Best Estimate Loss of Coolant Accident Analysis", March 1998.

CE Response 16:

[

]^{a,b,c}

[ ]

a, b, c

[

]^{a,c}

These results substantiate the argument on page 28 and demonstrate that the overprediction of the specific heat data [ ]^{a,c} by the ZIRLO™ specific heat model has an insignificant effect on the LBLOCA PCT. In particular, the sensitivity analysis showed that, when the specific heat data is represented, there is an increase in cladding temperature during blowdown when the cladding temperature is passing through the subject temperature range. [

]^{a,c}

References

16-2 **CENPD-132, Supplement 4-P-A, "Calculative Methods for the CE Nuclear Power Large Break LOCA Evaluation Model," March 2001.**

17. Section 4.6 (Page 24) – The measurements of high temperature creep rate plotted in Figure B.14.1 are implied to be determined from the secondary or steady-state creep rate. However, page A-6 in Appendix A explanation of how the creep rates were determined at and below 1183 °K for this figure appear to suggest that the creep rates are based on primary creep, i.e., tangential slope of strain versus time plot starting at zero strain. Please provide an example of how the strain rates were determined from an actual strain versus time plot for temperatures equal to and below 1183 °K and those at 1273 °K.

Response 17:

[

]^{a,c}

Figure 17.1 – Optimized ZIRLO™ Creep Test – 1093 K 20 MPa

a,b,c

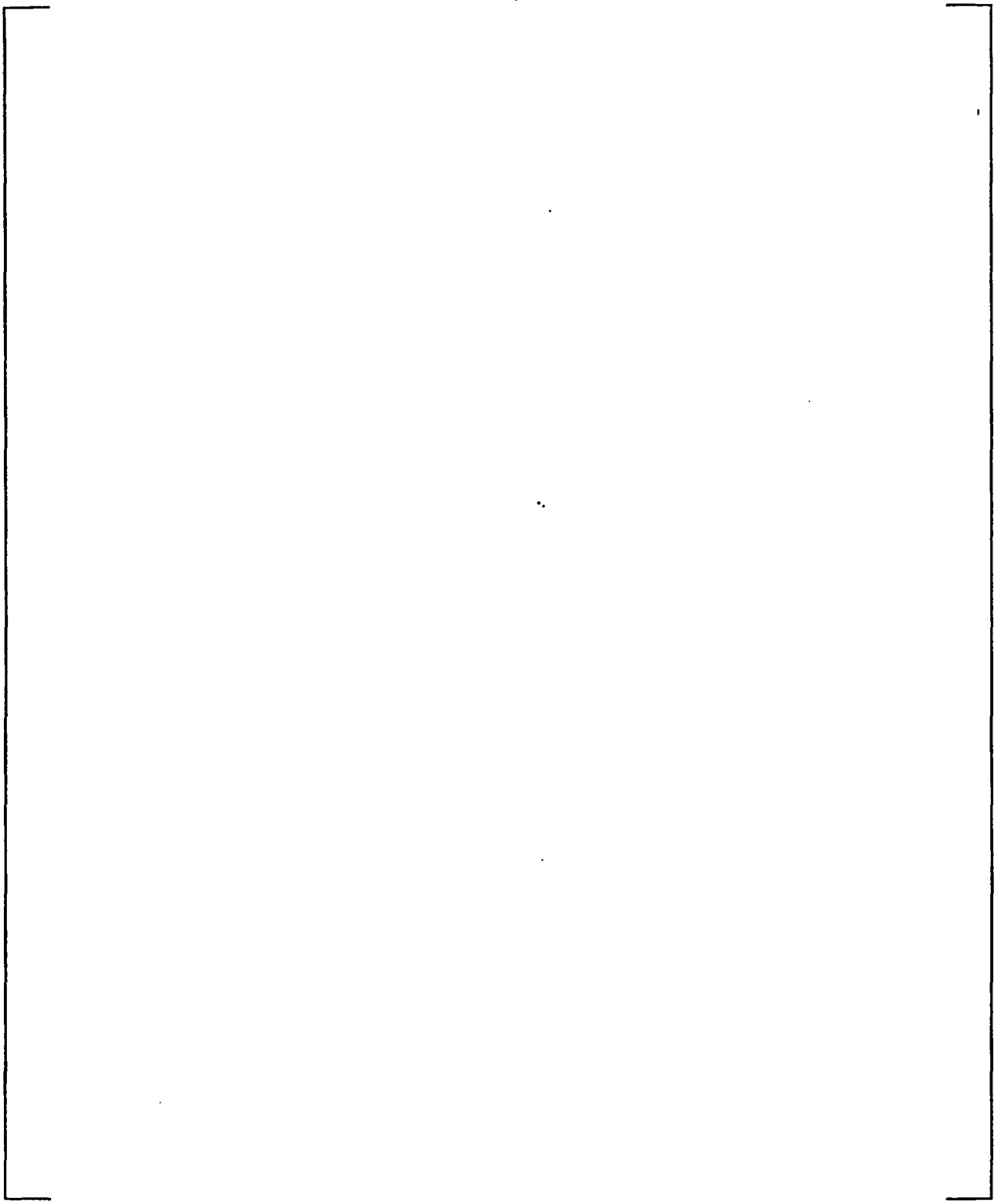

Figure 17.3 – Optimized ZIRLO™ Creep Test – 1273 K 4 MPa

a,b,c

18. Appendix B -- The tin concentrations of the Optimized ZIRLO™ data were not always provided in Appendix B. What were the tin concentrations of the Optimized ZIRLO™ properties data provided in Appendix B for emissivity, thermal expansion, high and low temperature thermal creep, fatigue, single rod burst, high temperature oxidation, and ring compression tests.

Response 18:

Refer to Response 14. As reported in section 3.1, [

]^{a,c}. Both the lots were for tested for emissivity, diametral thermal expansion, low and high temperature thermal creep, fatigue, high temperature oxidation and ring compression tests. For single rod burst tests, lot Q40-1113 was used. For axial thermal expansion, lot Q40-1114 was used.

19. Appendix B.14 - The high temperature creep data demonstrate that the current high temperature creep model overpredicts cladding strain [ ]^{a,c} in a steam atmosphere. What are the consequences if cladding strains are overpredicted in the large and small break analysis? Is this always conservative or are there instances where this could result in non-conservative results?

Response 19:

It cannot be stated that over-predicting the cladding strain prior to burst is always conservative for large and small break LOCA analyses. But the degree of over-prediction observed at [ ] [a,b,c] is not indicative of the expected effect on large and small break LOCA analysis results, and it was decided to conduct some additional tests under conditions more typical of a licensing-basis LOCA transient. [

] [a,b,c]

Predictions of the tests were obtained using a computer program adapted from the LOCBART swelling and rupture models for ZIRLO™ cladding. These models calculate the change in clad diameter vs. time due to thermal expansion, mechanical strain, and high-temperature creep, and can be readily compared against the test results which include transient measurements of the clad outside diameter. [

] [a,b,c]

Figure 19-1

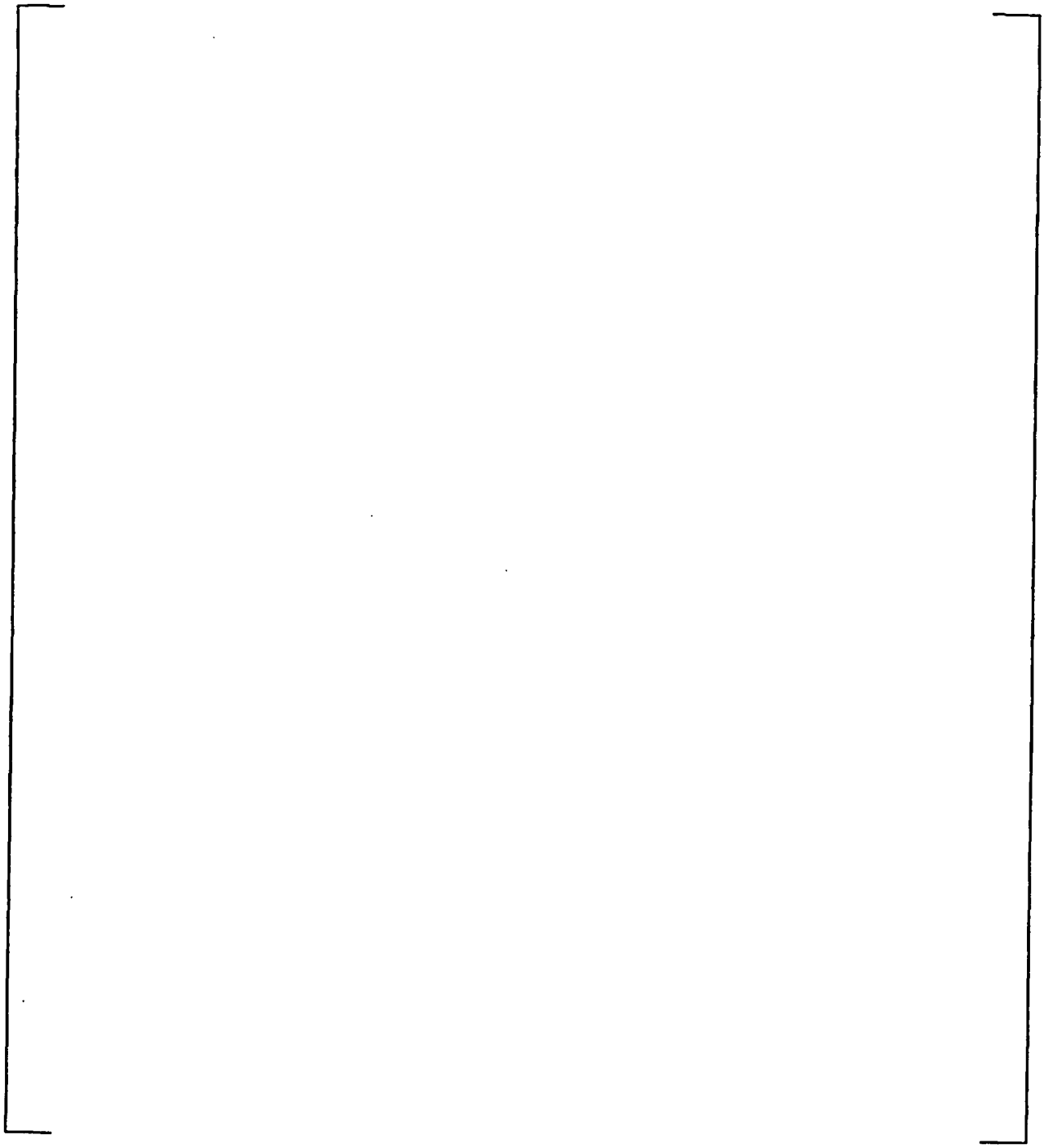

a,b,c

The swelling and burst data obtained with [

]$^{a, b, c}$ The following discusses, in general, how the high temperature creep model is integrated within the Westinghouse Appendix K LOCA evaluation models, using LOCBART as an example.

LOCBART is used to calculate the hot rod and hot assembly thermal responses during the large break transient. The largest axial noding used is 6 inches, with the blockage region and the limiting PCT regions modeled using 3-inch axial noding. The rod internal pressure is calculated as a function of time, accounting for changes in temperature in the various gas regions (plenum, gap and stack), and fuel rod dimensions (e.g., cladding plastic deformation due to high temperature creep). Plastic deformation, or swelling, is allowed to occur at any elevation where the cladding temperature and differential pressure are high enough to cause high temperature creep. [

]$^{a, c}$ When cladding burst occurs, the rod internal pressure is relieved, and the high temperature creep process is terminated.

[

]$^{a, c}$

20. Section 4.6 - The non-linear increase in ZIRLO™ thermal conductivity observed [

] [a,c] Please explain. What were the heating rates of the laser diffusivity measurements?

Response:

The thermal conductivity does have a non-linear change near the temperature of 900 C [ ][a, b, c]. To better understand the temperatures related to the change a plot was made of the incremental slope of the lines between the data points of the thermal conductivity data in Table B.3-1 of Appendix B to WCAP-12610-P-A. The following figure 20.1 shows the results of that calculation that focuses on the temperatures at which the thermal conductivity rate is changing. The chart indicates that the thermal conductivity rate with temperature starts to change at about [ ][a, b, c]. This temperature range is similar to the start of the alpha to alpha + beta temperature range reported in section B.6 and observed in the specific heat measurements in section B.2.

Figure 20.1

[ ] a,b,c

The method used for the thermal conductivity/diffusivity measurements follows ASTM E1461 and involves relatively fast incremental heating rates. The sample is preheated to the test temperature and then pulsed with a laser of known energy. The temperature rise on one face of the sample disk is about 30° C for a few milliseconds and on the back face of the disk the temperature rise is about 1.5 °C. The relative heating rates will result in some minor differences in the observed phase transitions. To obtain a more accurate phase change profile using this technique would require data points at smaller temperature intervals. However, the data is consistent and shows that the thermal conductivity rate change is related to the phase change.

21. Section 4.5 - It is noted in this section that the differences in specific heat between Zr-4 and ZIRLO™ have no or negligible effect on non-LOCA analyses. However, there are several material property data for Optimized ZIRLO™ that are different from the model used in Westinghouse and CE evaluation models by more than 10%. Are there other accidents besides large break LOCA, e.g., small-break LOCA, Locked Rotor/Sheared Shaft, and Rod Ejection events, where an underprediction of clad thermal conductivity above 1000 °C, or an overprediction in clad emissivity, or an underprediction of clad thermal expansion have an impact on the calculated results? What is the cumulative impact of all these differences including specific heat on large break LOCA and other accident analyses?

Response

As discussed in Sections 4.6.1 and 4.6.2 of the Topical Report, the differences between the emissivity models and the Standard/Optimized ZIRLO™ data are mostly attributed to the testing environment, and therefore should not be assessed against current licensing-basis analysis results. For thermal conductivity, thermal expansion, and specific heat, additional sensitivity calculations were completed using LOCBART and SBLOCTA to demonstrate the effect of differences between the models and data on results. The changes to the models are described below, followed by the sensitivity calculations which demonstrate an insignificant effect on the calculated peak cladding temperature.

For thermal conductivity, the current ZIRLO™ model shown in Figure 4.6.1-2 of the Topical Report was replaced by a table of the Optimized ZIRLO™ points from Table B.3-1 of the Topical Report. (Note that the first temperature point differs slightly due to rounding.) For diametral thermal expansion, the current expansion coefficient of [ ]^{a,c} was increased to [ ]^{a,b,c} based on the value used in the CE model sensitivity calculation described in Section 4.6.2 of the Topical Report. (Note that axial thermal expansion is not modeled in LOCBART and SBLOCTA.) For specific heat, the current ZIRLO™ model (which is now based on the Standard ZIRLO™ "heating" data from Table B.2-1 of the Topical Report, per Reference 21-1) was replaced by a table of 26 points based on the Optimized ZIRLO™ "heating" data from Table B.2-1 of the

Topical report. (See the Specific Heat part of Section 4.6.1 of the Topical Report for related information.)

The first case is a sample LOCBART transient with a burst-node-limited, early-reflood PCT. The base calculation (denoted as case (a)) modeled Standard ZIRLO™, and the sensitivity calculations modeled (b) Optimized ZIRLO™ thermal conductivity and thermal expansion, (c) Optimized ZIRLO™ specific heat, and (d) Optimized ZIRLO™ thermal conductivity, thermal expansion, and specific heat. Figure 21-1 compares the cladding temperature at the PCT elevation for the base case and case (d) and indicates a minimal effect on the overall transient behavior. Relative to the base case, the PCT increased by about [ ]^{a,b,c} for case (b), [ ]^{a,b,c} for case (c), and [ ]^{a,b,c} for case (d), all of which are insignificant despite the over-sensitivity of LOCBART to changes for this type of transient. Figure 21-2 compares the cladding temperature at the PCT elevation for all four cases near the PCT time and shows that most of the temperature increase results from the change in specific heat, which is consistent with the expected result given the relative importance of the specific heat vs. thermal conductivity/thermal expansion models in a large break LOCA transient.

The second case is a sample LOCBART transient with a late-reflood PCT. For this case, the four calculations described above resulted in a total variation in PCT of less than [ ]^{a,b,c}. Figure 21-3 compares the cladding temperature at the PCT elevation for the base case and case (d) and indicates a minimal effect on the overall transient behavior, which is consistent with the expected result for large break LOCA transients where the PCT occurs late in reflood.

The third case is a sample SBLOCTA transient. The base case was reanalyzed using the Optimized ZIRLO™ thermal conductivity, thermal expansion, and specific heat, resulting in a PCT decrease of about [ ]$^{a,b,c.}$ Figure 21-4 compares the cladding temperature at the PCT elevation and indicates a minimal effect on the overall transient behavior, which is consistent with the expected result for small break LOCA transients.

Based on these and other calculations that have been performed for the Optimized ZIRLO™ program, differences between the models and data for parameters such as thermal conductivity, thermal expansion, and specific heat have generally been found to produce a negligible effect on the analysis results. Similar effects are also expected for the CE LOCA evaluation models and non-LOCA transients such as locked rotor/sheared shaft and rod ejection, and updating the current ZIRLO™ models is generally not required to obtain an adequate prediction of Optimized ZIRLO™ performance. Somewhat larger effects were observed due to differences in specific heat for LOCBART transients with a burst-node-limited, early-reflood PCT, and were resolved as described in Reference 21-1 by updating the Standard ZIRLO™ specific heat model based on the "heating" data from Table B.2-1 of the Topical Report. (Note that the SBLOCTA specific heat model was also updated to maintain

consistency with LOCBART, with a negligible effect on results as indicated in Reference 21-1.)

Calculations using the Appendix K large break LOCA hot rod heat-up code LOCBART indicated an exaggerated sensitivity to specific heat for the small subset of plants with a peak cladding temperature (PCT) that occurs at the hot rod burst elevation coincident with the onset of entrainment in early reflood. This behavior is attributed primarily to excessive conservatism in the licensed method of transferring the core inlet flooding rate from BASH to LOCBART, and is exacerbated by the application of the overly-conservative Baker-Just correlation for zirconium-water reaction to both the inside and outside surfaces of the cladding at the hot rod burst elevation. [

Table 21-1: Optimized ZIRLO™ Specific Heat Model

a,b,c

]^{a,b,c}

A question has also been raised regarding the effect of variations in cladding specific heat on uncertainties for Best Estimate LOCA. Page 25-4-14 of Reference 21-2 states that "Uncertainty in cladding specific heat and conductivity is negligible relative to fuel uncertainties, and is ignored." In addition, the response to RAI #16 states that a HOTSPOT sensitivity calculation replacing the Standard ZIRLO™ specific heat model with a model based on the Optimized ZIRLO™ data "showed a 2.7°F increase in average PCT (from 2191.0°F to 2193.7°F) and a 1.7°F decrease in standard deviation (from 54.1°F to 52.4°F)", resulting in nearly identical 95th percentile PCTs of 2280.0°F and 2279.9°F for Standard and Optimized ZIRLO™ (respectively). Based on this information, no changes to the uncertainties for Best Estimate LOCA are required to account for the minor differences between the specific heats of Standard and Optimized ZIRLO™.

A question has also been raised regarding the effect of differences between OPTIN and Optimized ZIRLO™ properties on the swelling and rupture behavior for CE mechanistic DNB propagation analyses. For a plant that is transitioning from OPTIN to Optimized ZIRLO™, these effects would be adequately captured by completing mechanistic DNB propagation calculations using the swelling and rupture models described in Reference 21-3. This is consistent with information presented in Section 4.6 of the Topical Report, which has concluded that the swelling and rupture models for Standard ZIRLO™ can reasonably be applied to Optimized ZIRLO™ and need not be modified to reflect the new Standard ZIRLO™ data.

References

21-1. LTR-NRC-03-5, "U. S. Nuclear Regulatory Commission, 10 CFR 50.46 Annual Notification and Reporting for 2002", March 7, 2003.

21-2. WCAP-12945-P-A Volume I (Revision 2) and Volumes II-V (Revision 1), "Westinghouse Code Qualification for Best Estimate Loss of Coolant Accident Analysis", March 1998.

21-3. CENPD-404-P-A, "Implementation of ZIRLO™ Cladding Material in CE Nuclear Power Fuel Assembly Designs", November 2001.

Figure 21-1

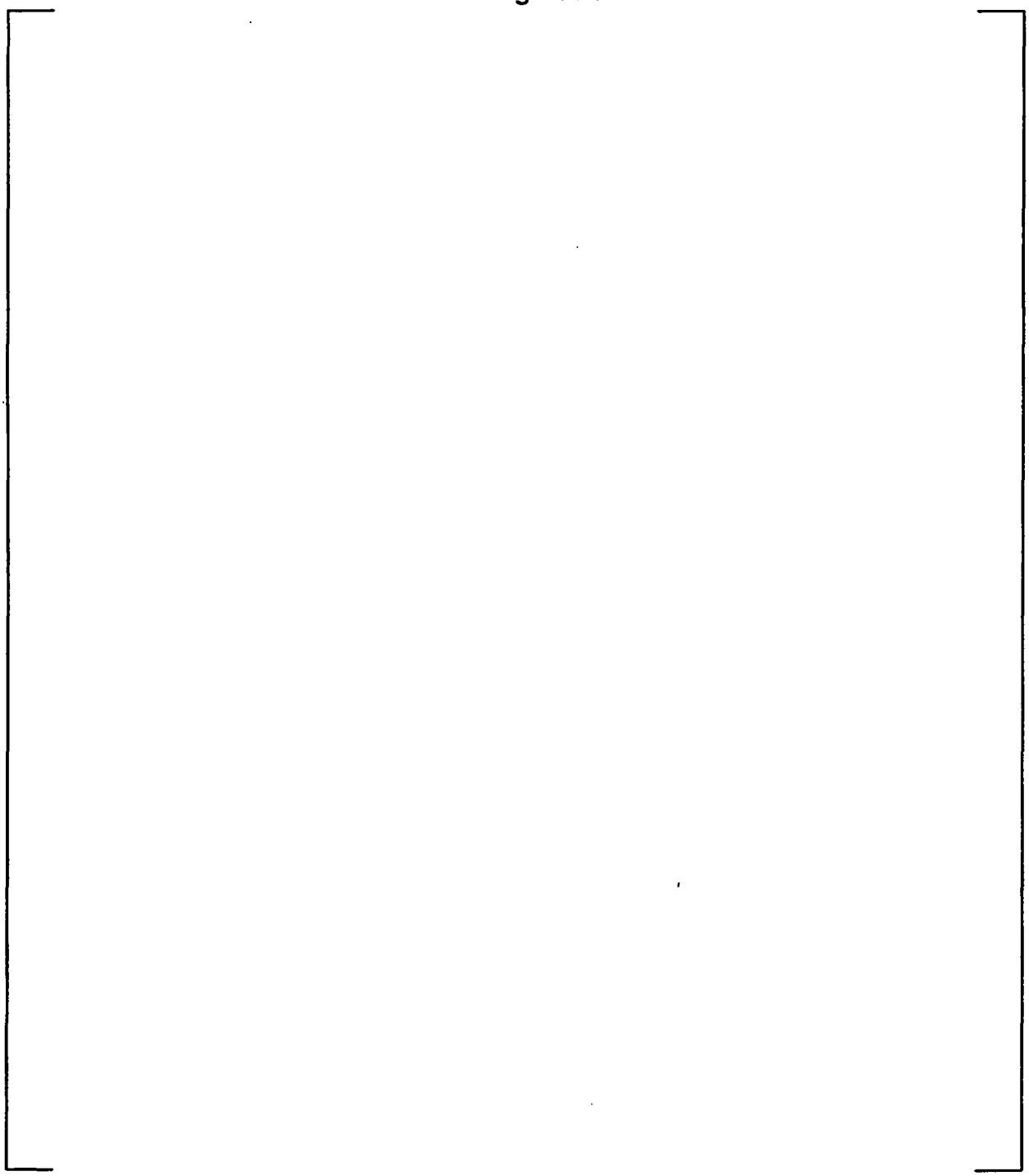

a,b,c

Figure 21-2

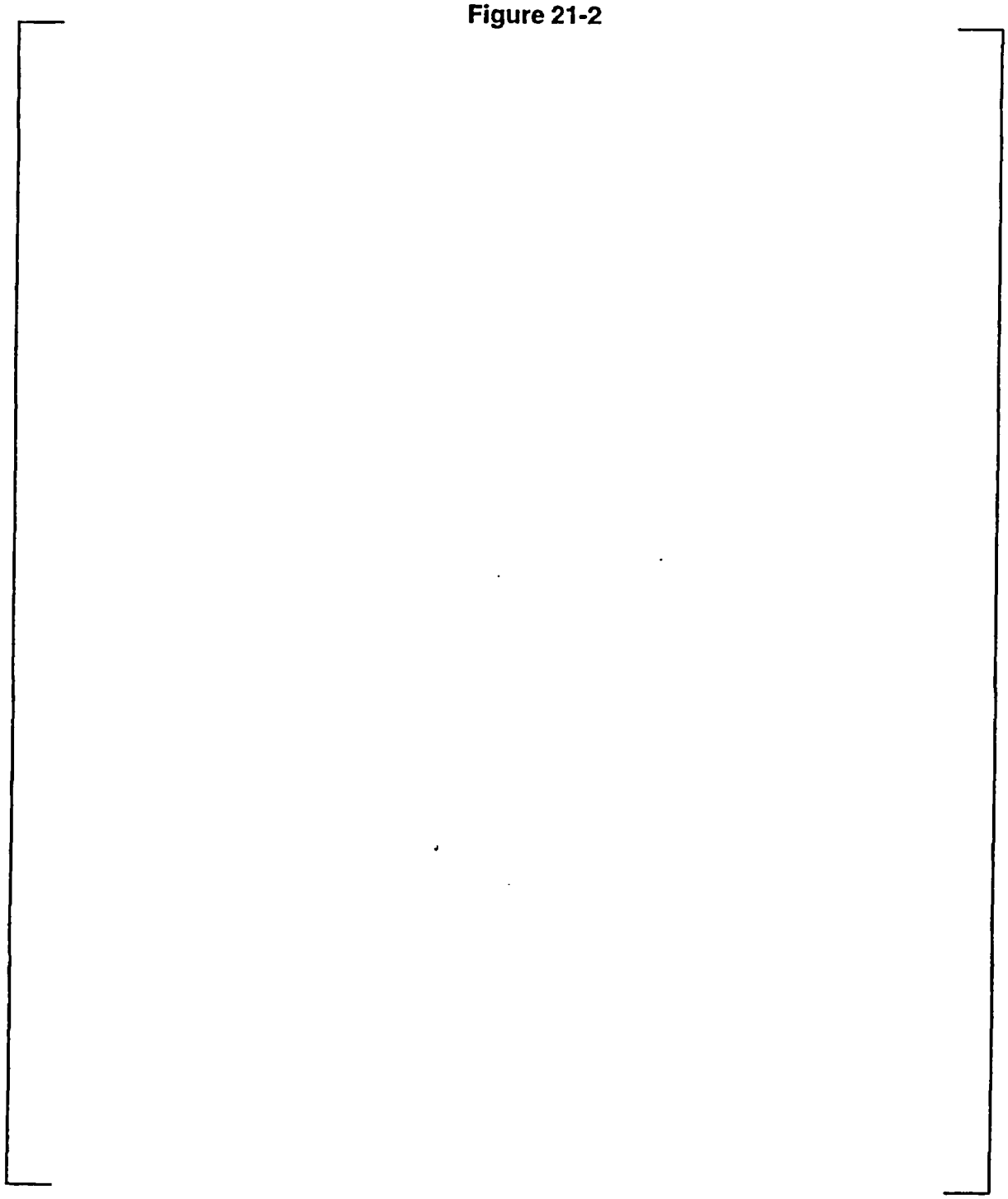

a,b,c

Figure 21-3

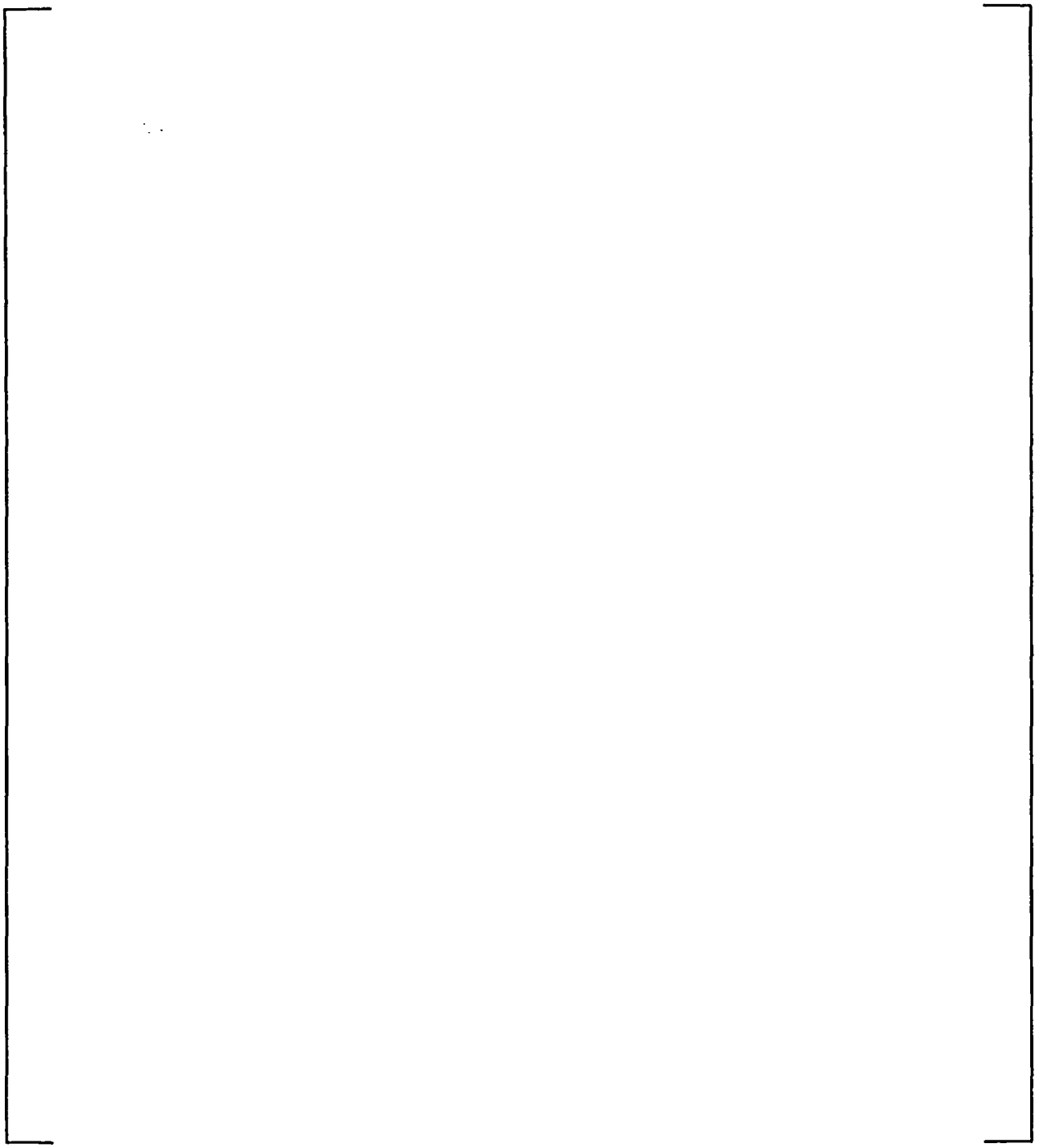

a,b,c

Figure 21-4

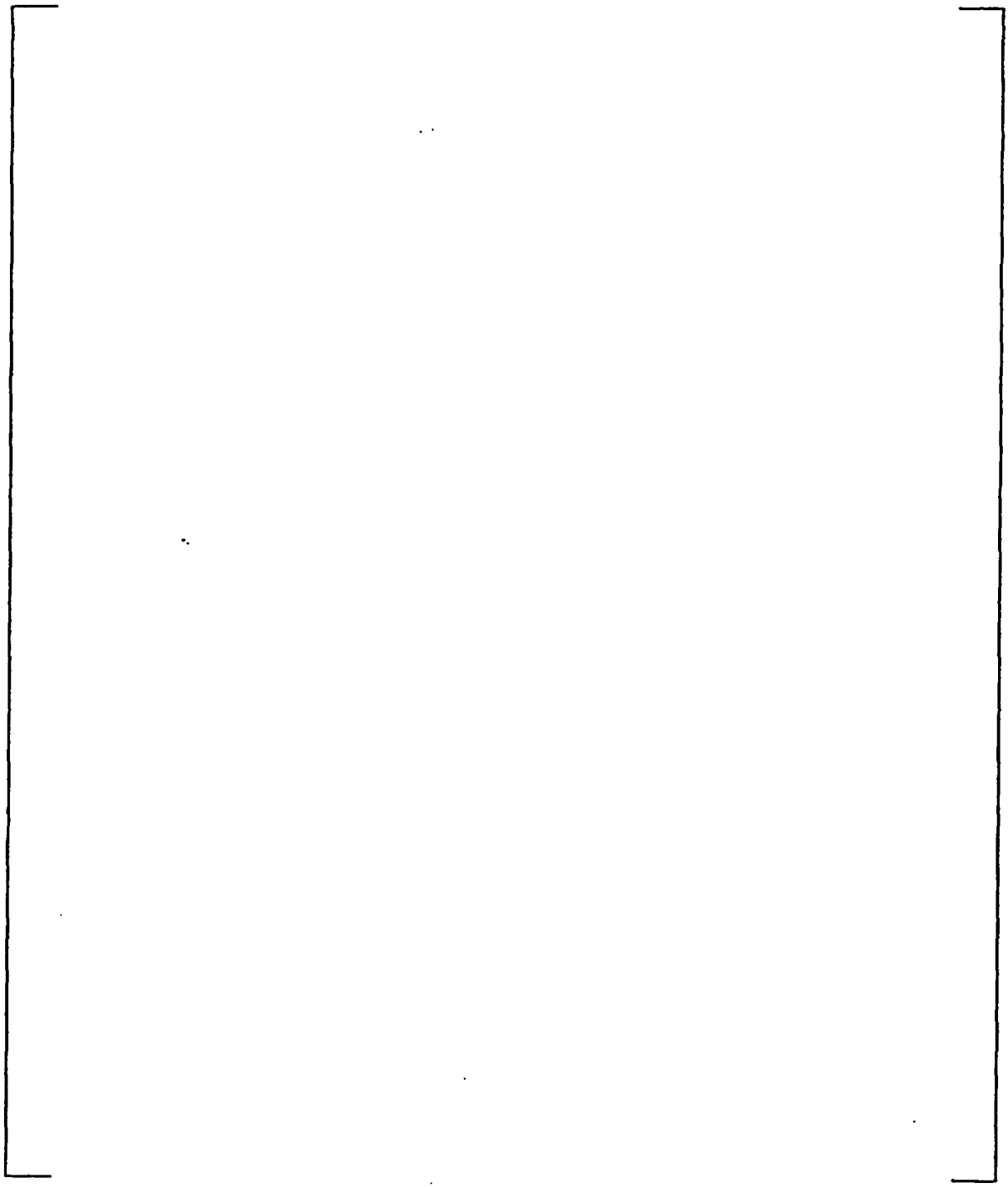

a,b,c

22. Section 4.6 - Please describe how flow assembly blockage is determined from rupture strain along with a description of the flow blockage models used in the Westinghouse and CE Evaluation models. What cladding strain values are assumed for the evaluation of equivalent cladding reacted (ECR) for LOCA analyses and provide an example with initial oxidation and oxidation following the LOCA?

Westinghouse Response 22:

For the Westinghouse evaluation models, the following describes the modeling of assembly blockage in Appendix K Small Break LOCA, Appendix K Large Break LOCA, Best Estimate Large Break LOCA, and SECY Large Break LOCA.

Appendix K Small Break LOCA

In SBLOCTA, assembly blockage is assessed based on burst of the hot assembly average rod, and is modeled [

]^{a,c}.

Appendix K Large Break LOCA

In LOCBART, assembly blockage is assessed based on burst of the hot assembly average rod, and is modeled as a non-uniform reduction in mass velocity in the vicinity of the burst elevation. To account for blockage in BART, the conservation equations were modified to include a source term representing the exit of steam from or entry of steam to the flow channel due to flow redistribution. As discussed in Section 3.2 of Reference 22-1, this source term was derived using an empirical expression for the normalized mass velocity vs. normalized elevation in the flow redistribution region, and depends on the mass velocity at the inlet of the flow redistribution region, the channel hydraulic diameter, the channel blockage fraction, the nodal and burst elevations, and the steam density. With this formulation, steam exits the channel in the lower portion of the flow redistribution region and re-enters the channel in the upper portion of the flow redistribution region, with a discrete approximation of a continuous profile that produces a minimum mass velocity slightly downstream of the hot assembly average rod burst elevation.

For a given axial node I that lies within the flow redistribution region, the flow redistribution model is activated when the following conditions are satisfied: [

]^{a,c}

The channel blockage fraction used with the flow redistribution model is based on Appendix B of NUREG-0630 (Reference 22-2) for Zircaloy-4 cladding at or below 1742°F; Figure 4 of Reference 22-3 for Zircaloy-4 cladding above 1742°F; or, Figure 5-4 of Reference 22-4 for ZIRLO™ cladding. Each of these references

describes the conversion from burst strain to assembly blockage, all of which use the basic approach outlined in NUREG-0630.

In the LOCBART modeling of assembly blockage, no direct credit is taken for the beneficial effects of droplet atomization, flow acceleration, or turbulence intensification that have been observed experimentally (e.g., Reference 22-5). As a result, assembly blockage leads to a local reduction in cladding-to-fluid heat transfer and a corresponding local increase in cladding temperatures, which is conservative relative to experimental results and can represent a substantial conservatism in the analysis when the peak cladding temperature occurs late in reflood.

Best Estimate Large Break LOCA
In the Best Estimate version of WCOBRA/TRAC, assembly blockage is assessed based on burst of the hot assembly average rod, and is modeled as an adjustment to the appropriate continuity and momentum cell areas. (See Section 7-4-2 of Reference 22-6.) The flow area reduction due to blockage is based on Figures 7-22 (Zircaloy-4) and 7-23 (ZIRLO™) of Reference 22-6. The conversion from burst strain to assembly blockage uses the basic approach outlined in NUREG-0630, as applied to the burst strain curves from Figures 7-18 (Zircaloy-4) and 7-20 (ZIRLO™) of Reference 22-6. HOTSPOT uses fluid conditions from WCOBRA/TRAC, and therefore does not require an explicit model for assembly blockage.

SECY Large Break LOCA
In the SECY version of WCOBRA/TRAC, assembly blockage is assessed based on burst of the hot assembly average rod, and is modeled as an adjustment to the appropriate continuity and momentum cell areas. (See Section 7-1-4 of Reference 22-7 and Sections 3-3-2 and 3-4 of Reference 22-8.) The flow area reduction due to blockage is based on NUREG-0630 (Reference 22-2) for Zircaloy-4 cladding and Table 3 of Reference 22-9 for ZIRLO™ cladding. Each of these references describes the conversion from burst strain to assembly blockage, using the basic approach outlined in NUREG-0630.

References

22-1. WCAP-8622, "Westinghouse ECCS Evaluation Model, October 1975 Version", November 1975.

22-2. NUREG-0630, "Cladding Swelling and Rupture Models for LOCA Analysis", April 1980.

22-3. ET-NRC-92-3746, "Extension of NUREG-0630 Fuel Rod Burst Strain and Assembly Blockage Models to High Fuel Rod Burst Temperatures", September 16, 1992.

22-4. WCAP-12610-P-A, "VANTAGE+ Fuel Assembly Reference Core Report", April 1995.

22-5. Erbacher, F. J., "Cladding Tube Deformation and Core Emergency Cooling in a Loss of Coolant Accident of a Pressurized Water Reactor", Nuclear Engineering and Design 103, pp. 55-64, 1987.

22-6. WCAP-12945-P-A Volume I (Revision 2) and Volumes II-V (Revision 1), "Westinghouse Code Qualification for Best Estimate Loss of Coolant Accident Analysis", March 1998.

22-7. WCAP-10924-P-A, Revision 2, "Westinghouse Large-Break LOCA Best Estimate Methodology; Volume 2: Application to Two-Loop PWRs Equipped with Upper Plenum Injection; Addendum 1: Responses to NRC Questions", December 1988.

22-8. WCAP-10924-P-A, Revision 1, "Westinghouse Large-Break LOCA Best-Estimate Methodology; Volume 1: Model Description and Validation; Addendum 4: Model Revisions", March 1991.

22-9. WCAP-13677-P-A, "10 CFR 50.46 Evaluation Model Report: WCOBRA/TRAC Two-Loop Upper Plenum Injection Model Updates to Support ZIRLO™ Cladding Option", February 1994.

What cladding strain values are assumed for the evaluation of equivalent cladding reacted (ECR) for LOCA analyses?

Westinghouse Response 22 (Cont'd):

For the Westinghouse evaluation models, the following describes the modeling of burst strain in Appendix K Small Break LOCA, Appendix K Large Break LOCA, Best Estimate Large Break LOCA, and SECY Large Break LOCA.

Appendix K Small Break LOCA

In SBLOCTA, the burst strain is taken as the [ ]^{a,c} (see Section 3-2-1 of Reference 22-8) and the value obtained using: Figure 5-3 of Reference 22-4 for ZIRLO™ cladding; or, the following equation for Zircaloy-4 cladding:

[ ]^{a,c}

where ΔP represents the cladding differential pressure at burst (psi).

Appendix K Large Break LOCA

In LOCBART, the burst strain is taken as the [ ]^{a,c} (see Section 3-2-1 of Reference 22-8) and the value obtained using Appendix B of NUREG-0630 (Reference 22-2) for Zircaloy-4 cladding at or below 1742°F; Figure 2 of Reference 22-3 for Zircaloy-4 cladding above 1742°F; or, Figure 5-3 of Reference 22-4 for ZIRLO™ cladding.

Best Estimate Large Break LOCA

The treatment of burst strain in HOTSPOT is described in Section 25-4-2-3 of Reference 22-6. As discussed therein, [

]^{a,c}.

SECY Large Break LOCA
In WCOBRA/TRAC, the burst strain is taken as the [
]^{a,c} (see Section 3-2-1 of Reference 22-8) and the value obtained using NUREG-0630 (Reference 22-2) for Zircaloy-4 cladding, or Table 3 of Reference 22-9 for ZIRLO™ cladding.

Provide an example with initial oxidation and oxidation following the LOCA.

Westinghouse Response 22 (Cont'd)
Consider a sample LOCBART calculation that produced the following results:

[

] **a,b,c**

[

]^{a,c} Transient results for the hot rod PCT and burst elevations are shown in Figures 22-1 (clad average temperature), 22-2 (local ECR), and 22-3 (clad outside diameter); note that the ECR computed by LOCBART includes both the transient and pre-transient values, with the latter being approximately zero for this near-beginning-of-life calculation.

Figure 22-1

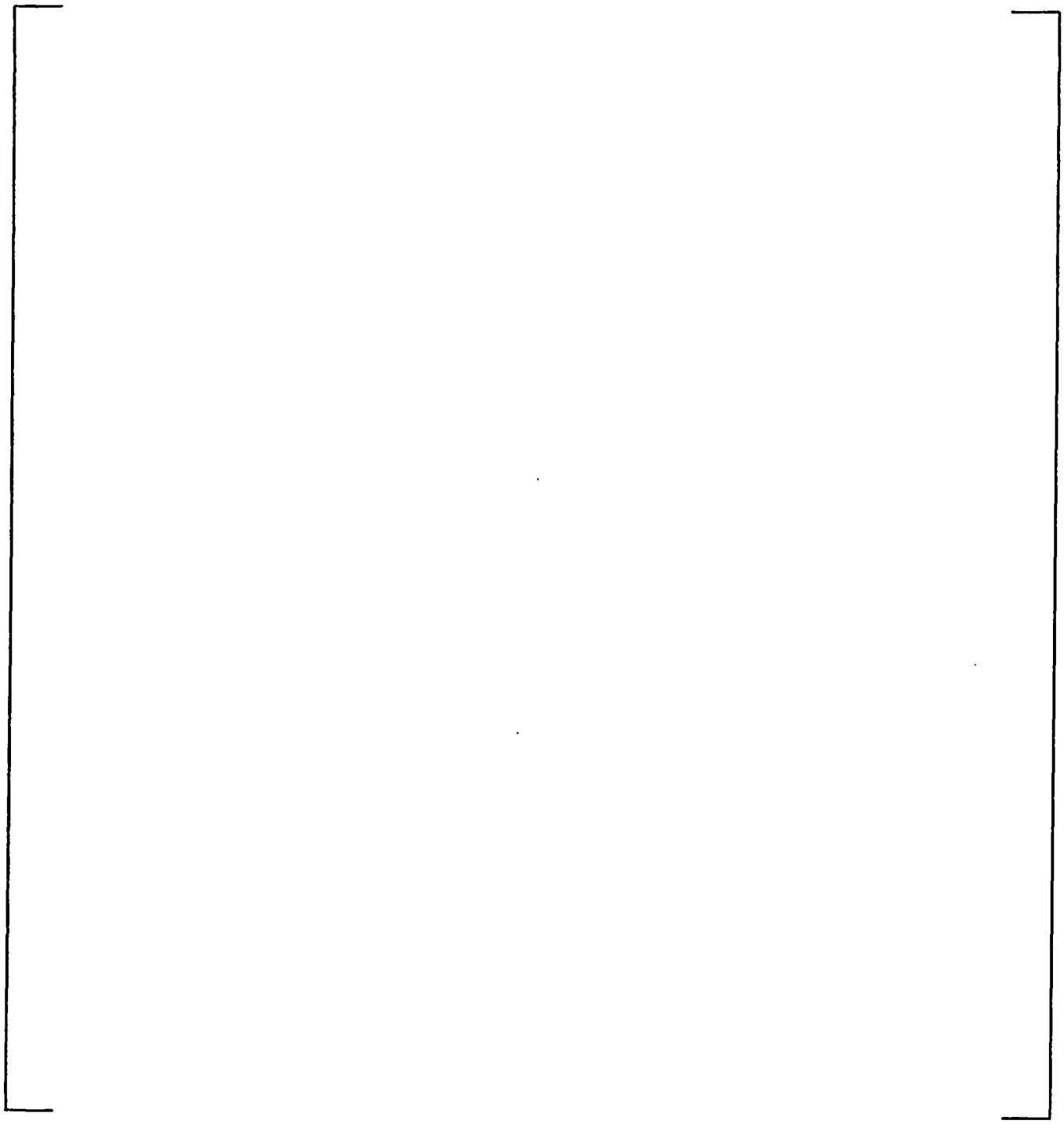

a,b,c

Figure 22-2

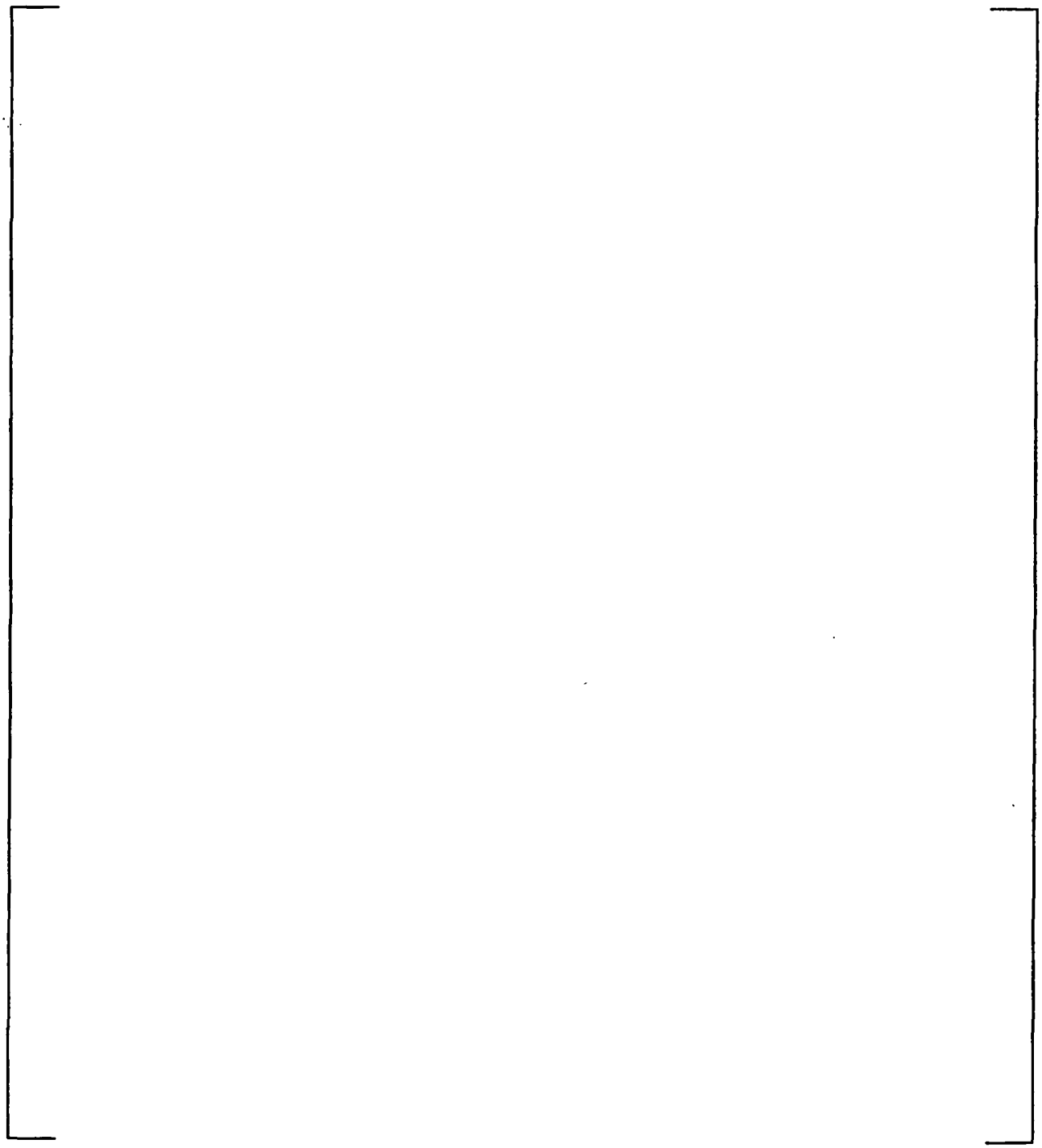

a,b,c

Figure 22-3

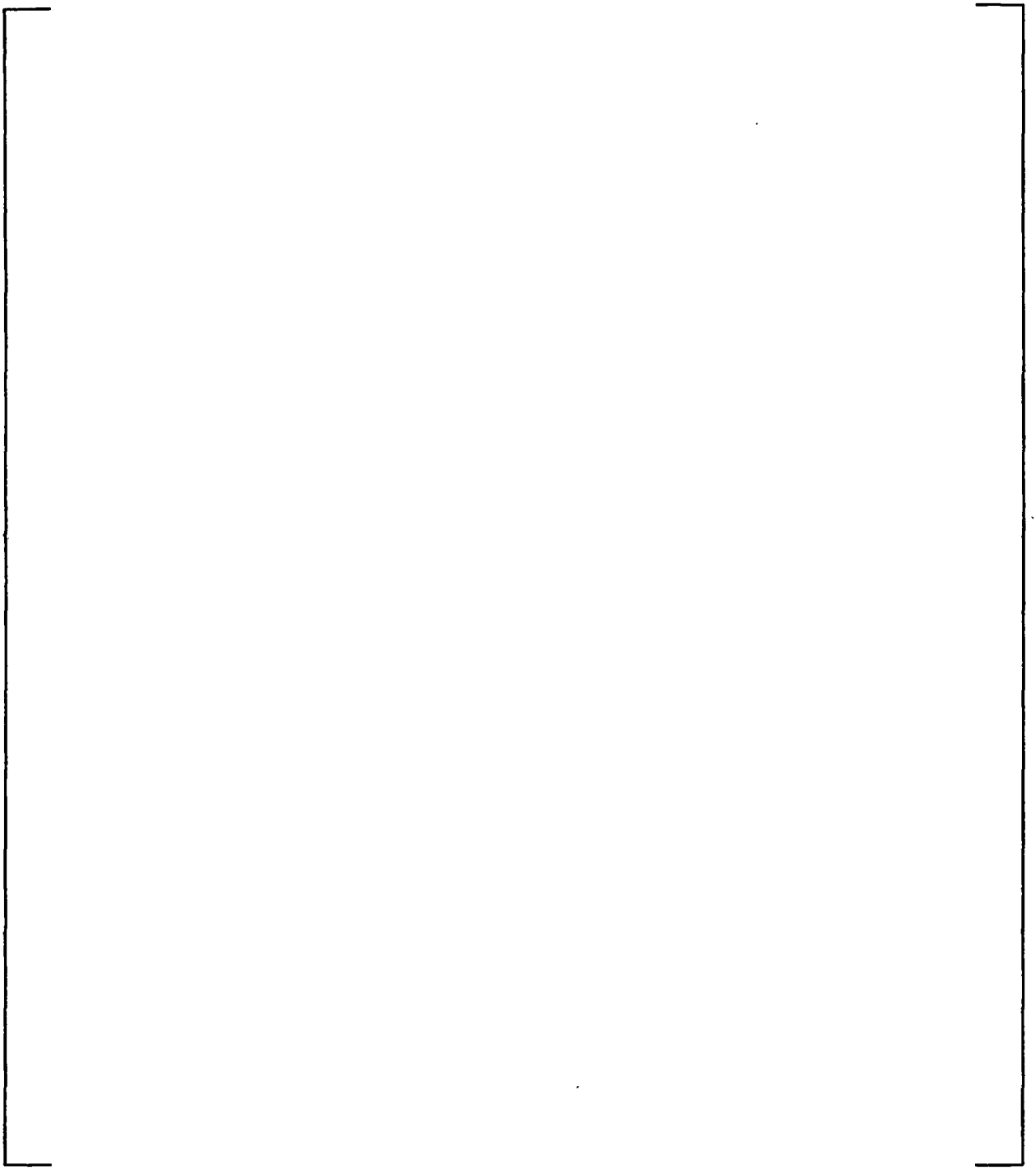

a,b,c

CE Response 22:

As described on pages 35 and 36 of Addendum 1 to WCAP-12610-P-A and CENPD-404-P-A, the CE evaluation models use the same cladding rupture strain and assembly blockage models for Optimized ZIRLO™ as are used for Standard ZIRLO™. The models are described in Sections 6.3.10 and 6.3.11 of CENPD-404-P-A (Reference 22-10). They consist of tables of rupture strain and assembly blockage versus rupture temperature (Tables 6.3.10.1-1 and 6.3.11-1 in CENPD-404-P-A). As noted in Section 6.3.11 of CENPD-404-P-A, the assembly blockage model was developed from [

]^{a,c}

The flow blockage model used in the CE LBLOCA evaluation model (i.e., the 1999 EM, Reference 22-11) is described in Enclosure 1-P-A to LD-81-095 (Reference 22-12). In the flow blockage model, the HCROSS computer code calculates the hot channel flow redistribution at and above the elevation of cladding rupture and the PARCH computer code calculates the hot rod steam cooling heat transfer coefficients. The steam cooling heat transfer coefficients are used by the STRIKIN-II computer code in the calculation of the hot rod cladding temperature at and above the elevation of cladding rupture after the core reflood rate decreases to less than 1 inch per second. Also, if cladding rupture is calculated to occur during blowdown, the blowdown hydraulics analysis performed by the CEFLASH-4A computer code is repeated to incorporate the impact of assembly blockage on the blowdown hydraulic response of the hot assembly. Note that in the 1999 EM, the HCROSS and PARCH computer codes have been integrated into the STRIKIN-II computer code (Section 2.7 of Reference 22-11). As described in Section 6.3.11 of CENPD-404-P-A, the CE SBLOCA evaluation model does not use a flow blockage model.

As part of the calculation of the cladding oxidation percentage (equivalent cladding reacted) in the CE evaluation models, the cladding rupture strain is used in the calculation of the amount of cladding oxidation at the elevation of cladding rupture (i.e., the cladding rupture node). As described in Section II.9 of the STRIKIN-II topical report (Reference 22-13) and Section 3.4.3 of the PARCH topical report (Reference 22-14), the cladding rupture strain is used to determine the inside and outside dimensions of the cladding rupture node. After rupture occurs, oxidation is calculated to occur on both the inside and outside surfaces of the cladding rupture node. Also, as noted in Section 6.3.10.1 of CENPD-404-P-A, the CE evaluation models do not [

]^{a,c} as is done in the Westinghouse Appendix K evaluation models.

Tables 6.5.1.3-1 and 6.5.1.3-2 of CENPD-404-P-A provide results of sample LBLOCA hot rod heat-up calculations for ZIRLO™ cladding for conditions of maximum initial fuel stored energy and maximum initial rod internal pressures, respectively. It is one of these two conditions that generally produce the limiting result in a LBLOCA analysis. As described in Section 4.6.2 of Addendum 1 to WCAP-12610-P-A and CENPD-404-P-A, the cladding models used for Standard ZIRLO™ are applicable to Optimized ZIRLO™. Therefore,

these sample calculations are also representative of Optimized ZIRLO™. The tables identify the cladding rupture strains and maximum cladding oxidation percentages that were calculated for sample cases. For the maximum initial fuel rod stored energy case for ZIRLO™ cladding, cladding rupture occurred at a cladding temperature of 1569°F. The resultant cladding strain and assembly blockage percentages were 33.2% and 24.1%, respectively. The maximum cladding oxidation, which occurred at the cladding rupture node, was calculated to be 6.80%. The value includes an initial cladding oxidation percentage of approximately 0.05%, which corresponds to the value associated with the initial cladding oxidation thickness used in the CE evaluation models. The corresponding results for the maximum initial rod internal pressure case are as follows: rupture temperature, 1454°F; cladding strain, 53.0%; assembly blockage, 40.2%; maximum cladding oxidation, 5.11%.

References

22-2 NUREG-0630, "Cladding Swelling and Rupture Models for LOCA Analysis," April 1980.

22-10 CENPD-404-P-A, Rev. 0, "Implementation of ZIRLO™ Cladding Material in CE Nuclear Power Fuel Assembly Designs," November 2001.

22-11 CENPD-132, Supplement 4-P-A, "Calculative Methods for the CE Nuclear Power Large Break LOCA Evaluation Model," March 2001.

22-12 Enclosure 1-P-A to LD-81-095, "C-E ECCS Evaluation Model Flow Blockage Analysis," December 1981.

22-13 CENPD-135P, "STRIKIN-II, A Cylindrical Geometry Fuel Rod Heat Transfer Program," August 1974.

22-14 CENPD-138P, "PARCH, A FORTRAN-IV Digital Program to Evaluate Pool Boiling, Axial Rod and Coolant Heatup," August 1974.

23. Section B.3 --- What specific heat function was used to reduce the diffusivity data to thermal conductivity? Was a different specific heat function used for heatup versus cooldown diffusivity data?

Response 23:

Discrete values were used, derived from the separate specific heat measurements. Changes in enthalpy attributable to phase changes were subtracted by smoothing visually across the phase transitions. Phase transition enthalpy is eliminated because the energy absorbed (or released) in phase transitions is unavailable for diffusion. Separate cooldown diffusivity data were not collected. Except for hysteresis in the phase transitions, there is no reason to expect that thermal diffusivity, specific heat, or thermal conductivity should vary as a function of whether the specimen is heating or cooling.

The values used are shown in the following table. It may be seen that the specific heat is not a strong function of temperature when enthalpy changes due to phase transitions are removed.

[ ] **a,b,c**

24. Section B.6 - The $\alpha \rightarrow \alpha + \beta$ transformation temperature data appears to show a dependence on tin content [ ] [a,c] such that there is a decrease in transformation temperature with a decrease in tin content. Why is this decrease not modeled?

Response 24:

The $\alpha \rightarrow \alpha + \beta$ transformation temperature is not explicitly modeled in the Non-LOCA or LOCA codes and methods, and only affects the analysis results through its influence on parameters that are explicitly modeled such as specific heat. For these parameters, the evaluations of Sections 4.5 and 4.6 have concluded that the Standard ZIRLO™ models can reasonably be applied to Optimized ZIRLO™, including any implicit effects due to the apparent reduction in the $\alpha \rightarrow \alpha + \beta$ transformation temperature.

What were the heating and cooling rates for the dilatometry and DSC measurements used to determine the $\alpha \rightarrow \alpha + \beta$ transformation temperature?

Response:

The heating and cooling rate for dilatometry was 3 °C/min.
The heating and cooling rate for specific heat (DSC) was 10 °C/min.

25. Sections B.7 & B.8 - The mechanical property data for microhardness, yield strength and ultimate yield strength of unirradiated Optimized ZIRLO™ is [ ] [a,c] lower than for standard ZIRLO™ at normal reactor operating conditions. It is also implied that irradiation hardening will decrease this difference such that there will not be a significant difference between these two materials. It is also implied that the difference in failure strains between Optimized and standard ZIRLO™ will also be reduced with irradiation. How can this claim be substantiated if there are no mechanical property tests on irradiated Optimized ZIRLO™? Are irradiation hardening effects accounted for in the properties for Optimized ZIRLO™? If so, how is this done without irradiated data?

Response 25:

Irradiation hardening is a known mechanism in Zirconium based alloys. An early review of this is found in Reference 1 where it is shown that the majority of the irradiation hardening effects develop early in the initial cycle of fuel operation. The hardening effect occurs with the displacement of lattice atoms under the fast neutron flux. Because it is basically a displacement of the matrix atoms and subsequent formation of microstructure changes such as dislocations , the irradiation hardening mechanism is relatively independent of minor alloy element level changes or final annealing conditions.

A specific example of the generic effects of irradiation hardening is found in the comparison of irradiated and un-irradiated ZIRLO and Zircaloy 4 materials. The following Table lists some nominal values of yield strength for these materials to show the relative changes in strength that occur in the materials with irradiation. The values may vary a small amount depending on the differing levels of fluence and hydrogen but the data still shows the similar response of Zircaloy 4 and ZIRLO to irradiation hardening. The

relatively large differences in the un-irradiated condition are significantly reduced or equalized with irradiation hardening.

The results in the comparison table show that even with different alloys and different heat treatments that the irradiation hardening has an overriding equalizing effect on the mechanical strength of zirconium based materials which have minor differences in alloy content. In the un-irradiated condition there are differences of 50 % to 200 % in yield strengths of the various materials but after irradiation the differences are less than 10 %.

a,b,c

In addition to the irradiation hardening effects the neutron fluence can also cause changes in the precipitate microstructure that can affect the material properties. For Optimized ZIRLO the only change in alloy chemistry is the tin level. Tin is in solid solution and is not a precipitate in the matrix. The precipitates are formed from the niobium and iron elements which are at the same levels in Optimized and standard ZIRLO. Therefore, there will be no difference in the precipitate structures of Optimized and standard ZIRLO for equivalent irradiation fluences. The equivalent mechanical property effects with irradiation and the equivalent precipitate microstructures with irradiation support the conclusion that standard ZIRLO irradiation data can be used to characterize the impacts of irradiation on Optimized ZIRLO and specific data on irradiated Optimized ZIRLO are not required.

As shown and discussed above, the irradiation hardening of Optimized ZIRLO will be same as observed for Zircaloy 4 and standard ZIRLO. For applications in beginning of life fuel rod design analysis that are sensitive to un-irradiated properties the un-irradiated mechanical properties will be used for Optimized ZIRLO fuel. For example un-irradiated properties will be used in evaluating early life limiting cases such as clad free standing.

Reference

25.1. " Effect of Irradiation on Strength , Ductility and Defect Sensitivity of Fully Recrystallized Zircaloy Tube"; Pettersson K. et al ; ASTM STP 681 Zirconium in the Nuclear Industry 1979, pp 155-173

26. Section B.7 - This section provides data that suggests there are [ ]^{a,c} differences in total elongation and failure strains in the longitudinal and circumferential direction between unirradiated Optimized and standard ZIRLO™. What tests were used to determine the failure strains in the circumferential direction? If ring tensile tests were used it has been demonstrated that this test method is not valid for determining failure strains because the strains are a function of specimen size, gauge length and ring test apparatus and, therefore, not a property measurement of failure strain. It is also known that the ring tests generally result in higher failure strains than other methods. Please provide additional discussion in this area. How was circumferential Young's modulus obtained, from the ring tests?

Response 26:

Circumferential Young's modulus was obtained from a split-D type mechanical test, in which two opposite sides of the tubing are loaded in circumferential tension.

Do the Westinghouse and CE evaluation models assume isotropic mechanical properties and, if so, what is used for Young's modulus for the isotropic analyses?

Westinghouse Response 26:

In the Westinghouse evaluation models, mechanical properties are either assumed to be isotropic or treated as having a simple directional dependence. This yields considerable simplification relative to a rigorous anisotropic treatment such as that described in Section 4.6 of Reference 26-1, and is considered to be adequate for the intended purpose given the minimal importance of these parameters in evaluation model calculations. Young's modulus (Y) is specified as a function of temperature (T), with the following equation used in LOCBART and SBLOCTA (Y in psi and T in °F):

[ ]^{a,c}

and the following equations used in WCOBRA/TRAC (Y in Pa and T in K):

T < 1094 K: [ ]^{a,c}

1094 K ≤ T ≤ 1239 K: [ ]^{a,c}

T > 1239 K: [ ]^{a,c}

A concern was raised regarding the adequacy of the LOCBART/SBLOCTA and WCOBRA/TRAC models for cladding elastic modulus at temperatures above 400°C. (Note that the LOCBART/SBLOCTA model is also used in the other Westinghouse Appendix K large and small break LOCA codes that consider cladding deformation, while the WCOBRA/TRAC model is not used in any of the other Westinghouse or CE LOCA or Non-LOCA codes.) The fuel rod swelling and burst processes in a licensing basis LOCA transient are driven primarily by plastic deformation and, to a lesser extent, thermal expansion. Elastic deformation of the cladding is a lower-order effect, and variations in the cladding elastic modulus would be expected to produce a negligible effect on the analysis results. As such, the models used in LOCBART/SBLOCTA and WCOBRA/TRAC are considered to be adequate for the intended purpose, and need not be modified for application at cladding temperatures above 400°C.

References

26-1.NUREG/CR-6150, Vol. 4, Rev. 2, INEL-96/0422, "SCDAP/RELAP5/MOD 3.3 Code Manual: MATPRO - A Library of Materials Properties for Light-Water-Reactor Accident Analysis", January 2001.

CE Response:

The CE evaluation models use models for mechanical properties (e.g. Young's modulus and Poisson's ratio) that are only applied in the radial direction. Sections 6.3.6 and 6.3.7 of CENPD-404-P-A (Reference 26-2) provide a general description of the use of Young's modulus and Poisson's ratio in the CE evaluation models. They are used in the calculation of the inside diameter of the cladding, which, in turn, is used in the calculation of the gap conductance and the gap pressure. Since the models for Young's modulus and Poisson's ratio are only applied in a single (i.e., radial) direction, characterization of the models as isotropic versus anisotropic is a moot point.

As described on page 33 of Addendum 1 to WCAP-12610-P-A and CENPD-404-P-A, the Young's modulus model described in Section 6.3.6 of CENPD-404-P-A is used for Standard ZIRLO™ and Optimized ZIRLO™. It is also noted on page 33 that the model and the data for Young's modulus in the circumferential direction for both Standard ZIRLO™ and Optimized ZIRLO™ are in reasonable agreement over the temperature range of the data. The model consists of an equation for temperatures less than or equal to [ ]^{a,c} and linear interpolation from a table of values for temperatures above [ ]^{a,c} The equation is as follows:

[ ]^{a,c}

where Young's modulus is in units of kpsi and T is cladding temperature (°F). The table used for temperatures above [ ]^{a,c} is as follows:

a.b.c

References

26-2 CENPD-404-P-A, Rev. 0, "Implementation of ZIRLO™ Cladding Material in CE Nuclear Power Fuel Assembly Designs," November 2001.

27. Section 4.2 -- What are the consequences to the evaluations of Sections 4.2 if the microhardness, yield strength, ultimate tensile strength and Young's modulus are 25% lower for Optimized ZIRLO™ than for standard ZIRLO™? What are the consequences to the evaluations of Section 4.2 if the failure strains are lower by 50% than for standard ZIRLO™?

Response

Microhardness is a surface property which plays a minor role in the contact gap conductance component for fuel-to-clad heat transfer in the fuel performance for Westinghouse CE models as described in Section 4.3.5.4 of CENPD-404-P-A. Microhardness is not a parameter in the Westinghouse models. A 25% lower microhardness value would result in a small increase in contact heat conductance but an insignificant increase in total gap conductance.

The yield and ultimate tensile strengths increase with irradiation. The cladding stress is calculated and compared to the yield and ultimate tensile strengths. As described in Section 4.2.1, the Westinghouse irradiated yield and ultimate strengths are used. The irradiation of the Optimized ZIRLO™ significantly increases the strength. A 25% reduction in un-irradiated strength would have little impact relative to the irradiated strength. However, Westinghouse CE uses the un-irradiated strength as a limiting clad stress criterion as described in Section 4.2.1. Although the available stress margin is reduced, sufficient conservatism exists to satisfy the criterion even if strength is reduced by 25%.

A reduction in Young's modulus would have an insignificant or a beneficial impact on clad stress which depends on the source of the loads. The clad stress is in equilibrium with clad pressure differentials and is independent of Young's modulus. Clad stress based on a rigid pellet thermal expansion

is based on a known strain. Conversion of this strain into a clad stress is proportional to Young's modulus. Therefore, a 25% reduction would result in a similar reduction in clad stress. A reduction in yield strength and Young's modulus under such conditions would compensate and result in no impact.

Failure strain data applicable to Section 4.2 is shown in Figure B.7-8. A 50% variation is consistent with the variation shown in this figure However, Optimized ZIRLO™ failure strain is higher than standard ZIRLO™. Failure strain is not used in fuel performance calculations given in Section 4.2, therefore a 50% reduction in the Optimized ZIRLO™ failure strain shown in Figure B.7-8 would have no impact on results or conclusions of Section 4.2.

28. Section B.9 - Thermal creep data are presented from unirradiated Optimized and standard ZIRLO™ at one temperature and stress demonstrating that there is little difference for these conditions. However, irradiation induced creep is significantly different from thermal creep with approximately an order of magnitude higher creep rates. In addition, there are several papers that demonstrate decreasing tin contents in Zr-4 result in a significant increase in creep rate (Reference 28.1). While thermal creep tests (out-of-reactor) sometimes give a qualitative measure of differences in irradiation induced creep rates between two materials this qualitative measure is not always a good measure of differences in irradiation creep. Therefore, please provide irradiation creep data to substantiate in-reactor performance.

References:

28.1 F.Garzarolli, H. Stehle, E. Steinberg, "Behavior and Properties in Power Reactors: A short Review of Pertinent Aspects in LWR Fuel", Zirconium in the Nuclear Industry; Eleventh International Symposium, ASTM STP 1295, 1996, pp. 12-32.

Response 28:

The use of out-reactor thermal creep data to determine in-reactor creep is based on the correlation between out-reactor and in-reactor creep. This correlation was developed using Westinghouse fuel rod data irradiated in BR-3 and confirmed with the results reported by the EPRI/B&W Zr-4 Program.

BR-3 CWSR ZIRLO

Westinghouse fabricated CWSR ZIRLO™ fuel rod tubing with different final pilger area reductions. Two lots of tubing were fabricated. One was made with a final area reduction of 77% and a second with a reduced value of 60%. The two tube lots received the same processing except for the final pilger area reduction. The only difference between the two lots was the amount of cold-work. Texture measurements indicated that the texture of the two tube lots was similar.

The material was tested out-reactor at the test conditions of [

]$^{a, b, c}$.

The results are shown in Figure 28.1. The tubing fabricated with the higher area reduction exhibits higher creep-out (higher tension strains). Figure 28.2 presents free-standing fuel rod creep-down data with rods fabricated with the two different final pilger area reductions. The rods fabricated with the higher area reduction exhibit higher creep-down (higher compression strains). Figure 28.3 presents both the in-reactor and the out-reactor data showing the negative of in-reactor creep-down on the y-axis versus the out-reactor creep-out on the x-axis. Note that an increase in out-reactor creep directly correlates with in-reactor creep.

Oconee-2 EPRI/B&W Zr-4

The EPRI/B&W Program investigated the behavior of Zr-4 both with out-reactor and in-reactor creep tests. (Reference 28.2) Three tube lots were tested out-reactor and in-reactor. One material heat of Sandvik Zr-4 was tested in the CWSR and RXA conditions (lots S-1 and S-2, respectively). One lot of NRG tubing was tested in the CWSR condition. In the case of lots S-1 and S-2, the processing was identical except for the final anneal. The final anneal resulted in both texture and dislocation density differences. In the case of lot V-1, the processing for this lot was considered to be different from lot S-1. Lot V-1 was considered to have a lower area reduction and lower Q-ratio processing because the final tubing exhibited less grain distortion and lower radial texture.

Figures 28.4 to 28.6 present the in-reactor data at a hoop stress of -12.5 ksi (-86 MPa) (Reference 28.3). The out-reactor results were reported as equation correlations (Reference 28.2). Figure 28.7 presents both the in-reactor and the out-reactor data showing the negative of in-reactor creep-down on the y-axis versus the out-reactor creep-out on the x-axis. Note that an increase in out-reactor creep directly correlates with in-reactor creep. This confirms the CWSR ZIRLO BR-3 results.

Application to Optimized ZIRLO™

The final CWSR anneal temperature used for Standard ZIRLO™ was modified for Optimized ZIRLO such that the [ ]$^{a, b, c}$ Sn Optimized ZIRLO™ exhibited the same out-reactor creep as Standard ZIRLO. This behavior is shown in Figure B.9-1 of reference 28.4. Based on the correlation between out-reactor and in-reactor creep, the irradiation creep of Optimized ZIRLO™ will be the same as for Standard ZIRLO.

References

28.2 David L. Baty, W.A. Pavinich, M.R. Dietrich, G.S. Clevinger and T.P. Papazoglou, "Deformation Characteristics of Cold-Worked and Recrystallized Zircaloy-4 Cladding," Zirconium in the Nuclear Industry: Sixth International Symposium, ASTM STP 824, 1984, pp. 306-339.

28.3 D.G. Franklin, G.E. Lucas and A.L. Bement, "Creep of Zirconium Alloys in Nuclear Reactors," ASTM STP 815, 1983, Appendix III.

28.4 Addendum 1 to WCAP-12610-P-A and CENPD-404-P-A Optimized ZIRLO, February 2003.

Figure 28.1

Figure 28.2

a,b,c

Figure 28.3

a,b,c

Figure 28.4

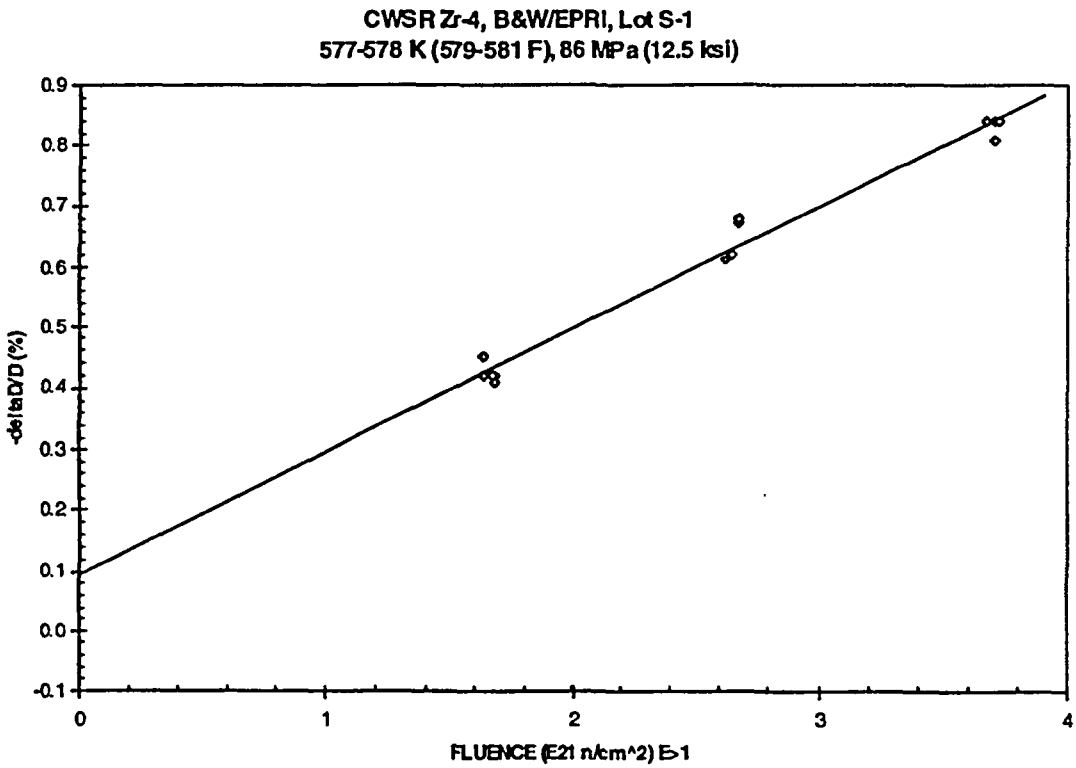
CWSR Zr-4, B&W/EPRI, Lot S-1
577-578 K (579-581 F), 86 MPa (12.5 ksi)
-deltaD/D (%)
0.9
0.8
0.7
0.6
0.5
0.4
0.3
0.2
0.1
0.0
-0.1
0
1
2
3
4
FLUENCE (E21 n/cm^2) E>1

Figure 28.5

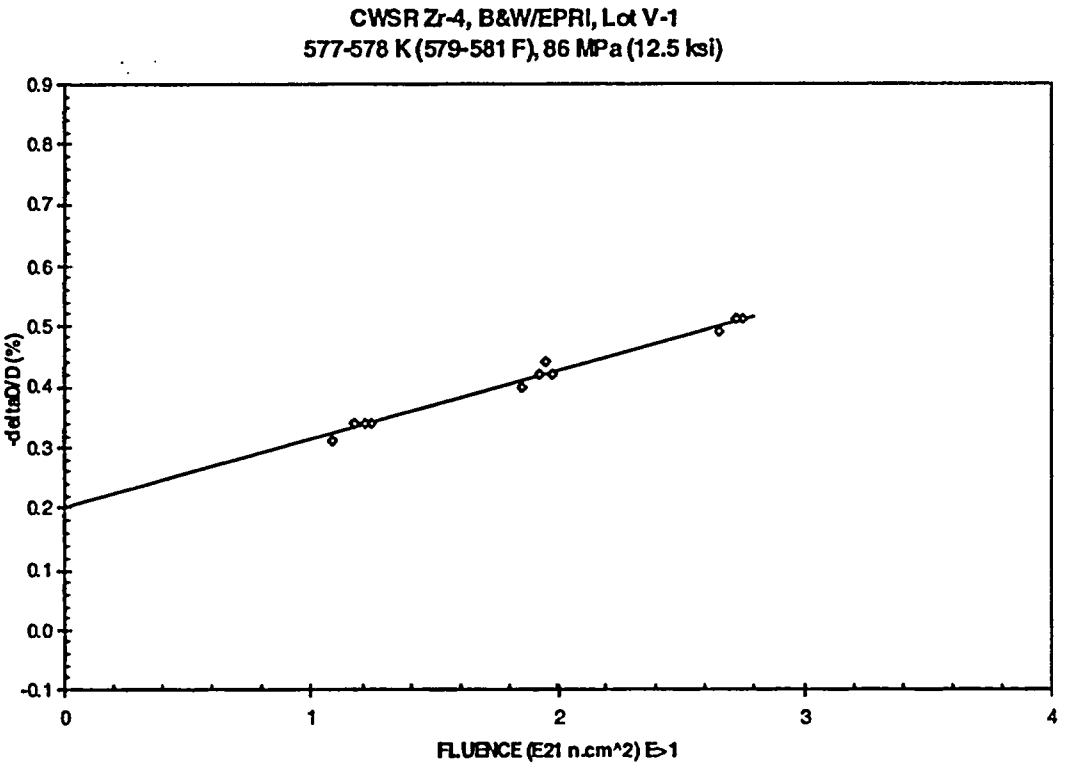
CWSR Zr-4, B&W/EPRI, Lot V-1
577-578 K (579-581 F), 86 MPa (12.5 ksi)
-deltaD/D (%)
0.9
0.8
0.7
0.6
0.5
0.4
0.3
0.2
0.1
0.0
-0.1
0
1
2
3
4
FLUENCE (E21 n.cm^2) E>1

Figure 28.6

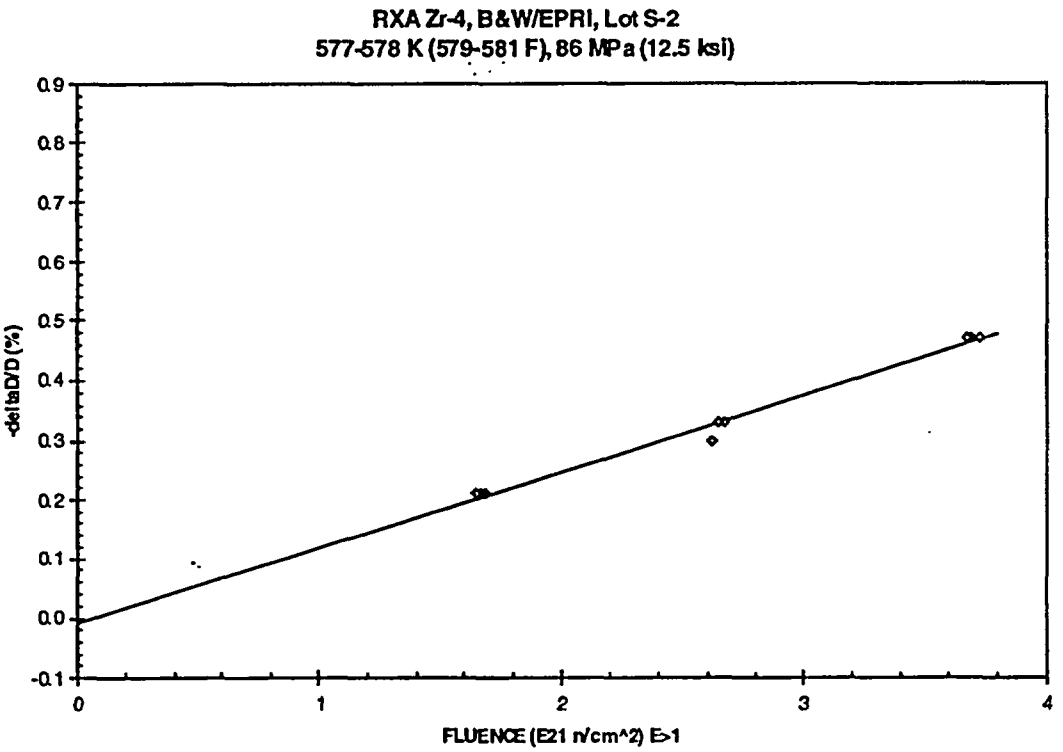
RXA Zr-4, B&W/EPRI, Lot S-2
577-578 K (579-581 F), 86 MPa (12.5 ksi)
-deltaD/D (%)
0.9
0.8
0.7
0.6
0.5
0.4
0.3
0.2
0.1
0.0
-0.1
0
1
2
3
4
FLUENCE (E21 n/cm^2) E>1

Figure 28.7

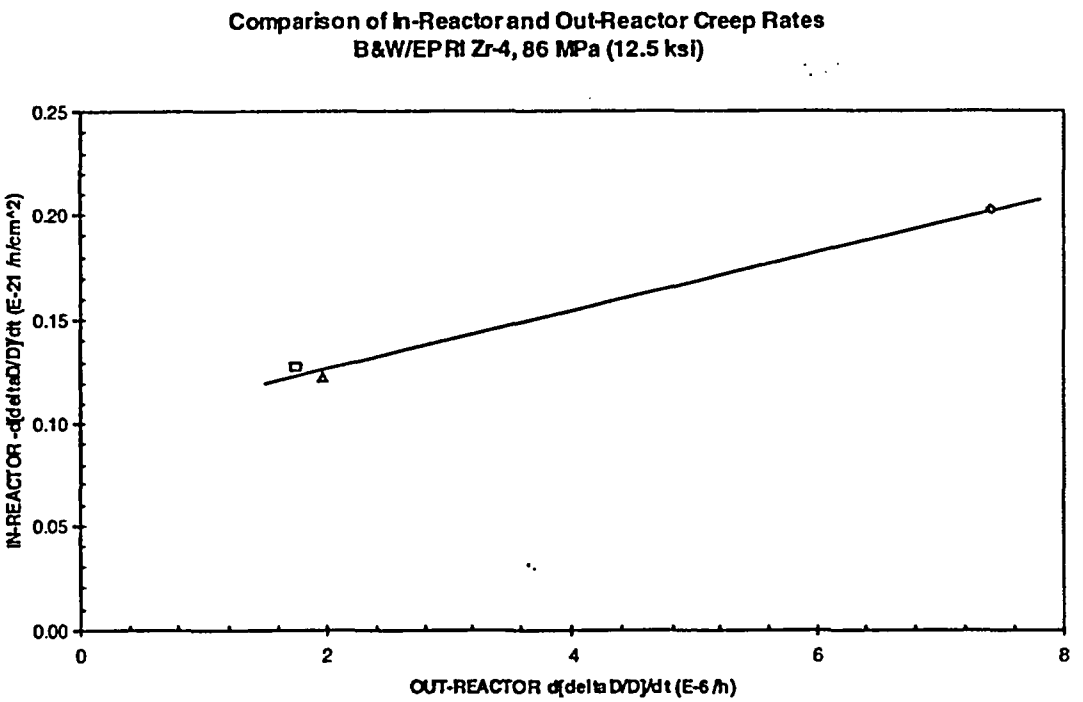
Comparison of In-Reactor and Out-Reactor Creep Rates
B&W/EPRI Zr-4, 86 MPa (12.5 ksi)
IN-REACTOR -d[deltaD/D]/dt (E-21 /h/cm^2)
0.25
0.20
0.15
0.10
0.05
0.00
0
2
4
6
8
OUT-REACTOR d[deltaD/D]/dt (E-6 /h)